9-15-2010

Prolonged Space Flight-Induced Alterations in the Structure and Function of Human Skeletal Muscle Fibres

Robert Fitts
Marquette University, robert.fitts@marquette.edu

S. W. Trappe
Ball State University

David Costill
Ball State University

Philip M. Gallagher
Ball State University

Andrew C. Creer
Ball State University

See next page for additional authors

Accepted version. *Journal of Physiology*, Vol. 588, No. 18 (September 15, 2010): 3567-3592. DOI.

Authors
Robert Fitts, S. W. Trappe, David Costill, Philip M. Gallagher, Andrew C. Creer, Patricia Colloton, Jim R. Peters, Janell Romatowski, J. L. Bain, and Danny A. Riley

Prolonged Space Flight-Induced Alterations in the Structure and Function of Human Skeletal Muscle Fibres

R. H. Fitts
Department of Biological Sciences, Marquette University Milwaukee, WI
S. W. Trappe
Ball State University, Muncie, IN
D. L. Costill
Ball State University, Muncie, IN
P. M. Gallagher
Ball State University, Muncie, IN
A.C. Creer
Ball State University, Muncie, IN
P. A. Colloton
Marquette University, Milwaukee, WI
J. R. Peters
Marquette University, Milwaukee, WI
J. G. Romotowski
Marquette University, Milwaukee, WI
J. L. Bain
Medical College of Wisconsin, Milwaukee, WI
D. A. Riley
Medical College of Wisconsin, Milwaukee, WI

Journal of Physiology, Vol. 588, No. 18 (September 2010): pg. 3567-3592. DOI.

Abstract

The primary goal of this study was to determine the effects of prolonged space flight (~180 days) on the structure and function of slow and fast fibres in human skeletal muscle. Biopsies were obtained from the gastrocnemius and soleus muscles of nine International Space Station crew members ~45 days pre- and on landing day (R+0) post-flight. The main findings were that prolonged weightlessness produced substantial loss of fibre mass, force and power with the hierarchy of the effects being soleus type I > soleus type II > gastrocnemius type I > gastrocnemius type II. Structurally, the quantitatively most important adaptation was fibre atrophy, which averaged 20% in the soleus type I fibres (98 to 79 μm diameter). Atrophy was the main contributor to the loss of peak force (P_0), which for the soleus type I fibre declined 35% from 0.86 to 0.56 mN. The percentage decrease in fibre diameter was correlated with the initial pre-flight fibre size (r = 0.87), inversely with the amount of treadmill running (r = 0.68), and was associated with an increase in thin filament density (r = 0.92). The latter correlated with reduced maximal velocity (V_0) (r = −0.51), and is likely to have contributed to the 21 and 18% decline in V_0 in the soleus and gastrocnemius type I fibres. Peak power was depressed in all fibre types with the greatest loss (~55%) in the soleus. An obvious conclusion is that the exercise countermeasures employed were incapable of providing the high intensity needed to adequately protect fibre and muscle mass, and that the crew's ability to perform strenuous exercise might be seriously compromised. Our results highlight the need to study new exercise programmes on the ISS that employ high resistance and contractions over a wide range of motion to mimic the range occurring in Earth's 1 *g* environment.

Introduction

The goals of the international space community are to conduct long-termed manned missions beyond the low earth orbit of the International Space Station (ISS). First, a number of issues regarding the deleterious effects of microgravity on human biology need to be addressed and resolved (Fitts *et al*. 2000; Trappe *et al*. 2009). It is clear from the last 40 years of space research, particularly studies conducted on the Skylab and MIR space stations and on mission STS-78 of the Space Shuttle Columbia (with the Life and Microgravity Spacelab, LMS), that limb skeletal muscle is particularly susceptible to microgravity-induced deterioration in both structure and function (Convertino, 1990; Fitts *et al*. 2000; Fitts *et al*. 2001). A consistent observation is significant atrophy of both upper and lower leg muscles

Journal of Physiology, Vol. 588, No. 18 (September 2010): pg. 3567-3592. DOI.

with the response occurring more rapidly in the triceps surae muscle group (ankle plantar flexors) than the anterior tibial group (ankle dorsal flexors) (Fitts *et al*. 2000). The primary cause of the decline in muscle mass appears to be the unloading of the skeletal and muscular systems rather than reduced activation. Support for this comes from the work of Edgerton *et al*. (2001) who found the total EMG activity of the tibialis anterior and soleus muscles of four crew members during the 17-day LMS space flight to be increased compared to pre- and post-flight values. The authors concluded that space flight on Shuttle missions is a model not just of space flight but rather microgravity plus the programmed work schedule. Despite the high EMG activity, the cross-sectional areas (CSAs) of the slow type I and fast type IIa fibres of the soleus muscles of the four crew members were on average 15 and 26% smaller post- compared to pre-flight (Widrick *et al*. 1999).

The composite data from Skylab, MIR and Shuttle flights suggest that the loss of limb muscle mass is exponential with the duration of flight, and that a microgravity steady state may be reached by approximately 180 days (Fitts *et al*. 2000). The loss in muscle force primarily reflects the decline in mass. Consequently, when single fibre force is expressed relative to cross-sectional area, there is little difference between pre- and post-flight values (Widrick *et al*. 1999; Fitts *et al*. 2000). In addition to the decline in muscle mass and peak force, crew members showed a depressed ability to generate power that was generally greater than the loss of force (Widrick *et al*. 1999; Fitts *et al*. 2000). For example, after 31 days in space, lower limb extensor force declined by 11%, while peak power was depressed by 54% (Antonutto *et al*. 1999). The latter was greater than the loss in single-fibre power after the 17-day LMS flight suggesting that factors other than atrophy contributed to the decline (Widrick *et al*. 1999; Fitts *et al*. 2000). Following the LMS flight, we found that the decline in peak power was partially protected by an increased maximal velocity (V_0) of both slow and fast fibres such that the velocity obtained at peak power was higher post-flight (Widrick *et al*. 1999). The elevated fibre V_0 was associated with and likely caused by an increase in myofilament lattice spacing that resulted from a reduction in thin filament density. It is unknown whether or not this adaptation persists with prolonged space flight or reflects a transient response to short duration flight.

Journal of Physiology, Vol. 588, No. 18 (September 2010): pg. 3567-3592. DOI.

A hallmark of space flight is that considerable variability in the extent of muscle atrophy and functional loss exists among crew members. For example, the crew members in this study showed calf muscle atrophy ranging from 1 to >20% and loss of maximal voluntary contractile force of the calf from 7 to 20% (Trappe *et al*. 2009). Similarly, Zange *et al*. (1997) observed muscle mass losses with 6 months in space to vary from 6 to 20%. Following the 17-day LMS flight, two crew members showed 2–3 times the reduction in peak force (mN) noted for the other two (Widrick *et al*. 1999). Besides mass and force, variability was also observed for Ca^{2+} sensitivity where the free Ca^{2+} required for half-maximal activation of soleus type I fibres post-flight ranged from no difference to 0.31 μmol more free Ca^{2+}.

The primary goal of this study was to use single, chemically skinned muscle fibre segments to determine the cellular effects of prolonged (~180 days) space flight aboard the International Space Station (ISS). An additional goal was to determine the extent to which the observed functional changes were fibre and muscle specific, and whether or not they could be explained by structural alterations. Changes in structure and function were to the extent possible related to differences in the type and amount of countermeasure exercise. To allow for scientific comparisons between the single fibre results described here and our recently published whole muscle data on the same subjects (Trappe *et al*. 2009), the letter code used for a given crew member was the same in both publications. The exercise countermeasure performed by each crew member was presented in detail in Trappe *et al*. (2009). The results were also compared to the known cell changes following short duration space flight.

Methods

Flight and subjects

The 10 crew members, five American astronauts and five Russian cosmonauts, who participated in this study flew aboard the International Space Station (ISS) from Increments 5 to 11 (2002–2005). All flights except for the first (Increment 5) originated and landed in Russia aboard the Russian Soyuz spacecraft. The crew of Increment 5 were ferried to and from the ISS on the Space Shuttle,

Journal of Physiology, Vol. 588, No. 18 (September 2010): pg. 3567-3592. DOI.

which lifted off and landed at Kennedy Space Center. The post-flight muscle samples for one crew member were damaged during shipment from Russia to the USA, and thus the data for this subject were not included. The subjects (n = 9) age, height, weight and days in space were 45 ± 2 years, 176 ± 2 cm, 81 ± 3 kg, and 177 ± 4 days (range = 161–192 days), respectively.

Prior to volunteering to participate in this study, all crew members were briefed on the project objectives and testing procedures by a member of the research team. Crew members were informed of the risks and benefits of the research and gave their written consent in accordance with the Human Subjects Institutional Review Boards at Marquette University, Ball State University, The Medical College of Wisconsin, and the National Aeronautics and Space Administration (NASA; Johnson Space Center). This study was conducted in accordance with the *Declaration of Helsinki*.

Pre- and in-flight exercise and nutritional profile

The pre- and in-flight exercise programmes of each crew member have been published elsewhere by our research team (Trappe *et al*. 2009). The crew members had access to a treadmill (Treadmill Vibration Isolation System; TVIS), two types of bicycle ergometers (Cycle Ergometer with Vibration Isolation System (CEVIS) and Velo, a Russian exercise device), and a resistive exercise device (Interim Resistive Exercise Device; iRED). The treadmill could be used in a passive (subject driven) or active (motorized) mode of operation. The exercise countermeasure programme was individually structured to allow for personal preference with guidance from staff within NASA and the Russian Space Agencies. A summary of the in-flight exercise is shown in Table 1. For more detailed information about the exercise prescription performed while on the ISS and individual aerobic and resistance exercise data profiles for each crew member see Trappe *et al*. (2009). The exercise profiles were determined from crew member logbooks and from downloaded analog data from the treadmill and cycle ergometer (Trappe *et al*. 2009). The in-flight diet was designed to meet the nutritional requirements for ISS missions as established by NASA and the Russian Space Agencies (Smith & Zwart, 2008). The

nutrient content of the pre- and post-flight foods was calculated using the Nutrient Data System for Research (Schakel *et al*. 1988).

Table 1. Summary of aerobic and resistance exercise performed while on the ISS

Cycle ergometer (CEVIS)		Treadmill (TVIS)		Resistance exercise (iRED)		
Time (min week^{-1})	Workload (W)	Time (min week^{-1})	Speed (mph)	Exercises	Frequency	Sets/reps
138 ± 26	126 ± 10	146 ± 32	3.2 ± 0.5	Squats	3–6 days week^{-1}	12–20
Range:	Range:	Range:	Range:	Heel raises	3–6 days week^{-1}	12–20
Little – 296	102 – 150	64 – 312	2.1 – 5.5	Dead lifts	3–6 days week^{-1}	12–20

For more detailed information about the exercise prescription performed while on the ISS and individual aerobic resistance exercise data profiles for each crew member, see Trappe *et al.* (2009).

Muscle biopsy

A muscle biopsy (Bergstrom, 1962) of ~80 mg was obtained from the mid-belly of the lateral head of the gastrocnemius and soleus muscles of each crew member prior to launch (L-55 ± 2) and on landing day (R+0) as described previously (Trappe *et al*. 2009). The post-flight biopsy was performed mid-to-late afternoon approximately 6–8 h after landing. The post-flight activity between landing and the biopsy was kept to a minimum, and during that time the crew members performed only light ambulatory activities.

Each biopsy sample was placed on saline-soaked gauze and divided longitudinally into several portions for subsequent structural and functional analyses exactly as described previously (Widrick *et al*. 1999). Two portions of each biopsy were placed in small vials containing cold (4°C) skinning solution (125 mm potassium propionate, 20 mm imidazole, 2 mm EGTA, 4 mm ATP, 1 mm $MgCl_2$, and 50% glycerol v/v, pH 7.0), and stored overnight at 4°C. The next day, the vials were packaged surrounded by frozen, water ice bottles in two boxes with each containing two vials (one soleus and one gastrocnemius sample), hand carried back to Ball State and Marquette Universities. Upon arrival, the bundles were placed in fresh skinning solution and stored at −20°C for up to 4 weeks. All contractile measurements on fibres from a given muscle were performed within 4 weeks of the initial bundle isolation. A third portion of each biopsy was pinned at a mild stretch and immersion fixed in a 0.1 m cacodylate buffer (pH 7.2) containing 4% glutaraldehyde and 2% paraformaldehyde with 5 mm $CaCl_2$. This sample was shipped overnight at 4°C to the Medical College of Wisconsin for osmium post-

Journal of Physiology, Vol. 588, No. 18 (September 2010): pg. 3567-3592. DOI.

fixation and embedding for electron microscopy as previously described (Riley *et al*. 1998). The fourth and fifth portions were frozen in liquid nitrogen and shipped in a liquid nitrogen dry shipper to Marquette University.

Solutions

The composition of the relaxing (pCa 9.0) and activating (pCa 4.5) solutions were derived with an iterative computer program (Fabiato & Fabiato, 1979) using the stability constants adjusted for temperature, pH and ionic strength (Godt & Lindley, 1982). All solutions contained (in mm): 20 imidazole, 7 EGTA, 14.5 creatine phosphate, 4 free ATP, and 1 free Mg^{2+}. Calcium was added as $CaCl_2$, and ATP as a disodium salt. Each solution had an ionic strength of 180 mm, which was controlled by varying the amount of KCl added. KOH was used to adjust the pH of the solution to 7.0. To prevent an increase in ADP or decline in ATP, we changed the activating solution after every two contractions. The activating and relaxing solutions were made fresh each week and stored at 4°C.

Single fibre preparation

This study involved the isolation and study of 1900 fibres with experiments conducted in the labs of Dr Fitts at Marquette and Dr Trappe at Ball State Universities. The procedures described here for the isolation and study of individual fibres were the same in both labs. While the single fibre systems used were similar, the equipment was not identical. Since the results obtained by each lab for all variables studied were similar, the data were pooled and presented here as one data set.

Single fibres were isolated and studied as described previously and briefly reviewed here (Widrick *et al*. 1999; Fitts *et al*. 2007). On the day of an experiment a muscle bundle was removed from the skinning solution and transferred to a dissection chamber containing pH 7.0 relaxing solution (4°C). An individual fibre was gently isolated from the bundle, transferred to an ~1 ml glass-bottomed chamber milled in a stainless steel plate. While submerged under relaxing solution (pH 7.0, 15°C), the ends of the fibre were carefully mounted

Journal of Physiology, Vol. 588, No. 18 (September 2010): pg. 3567-3592. DOI.

and attached between a force transducer (Cambridge model 400A; Cambridge Technology, Watertown, MA, USA) and servo-controlled direct-current position motor (Cambridge model 300B, Cambridge Technology). The position and speed of the motor was controlled by custom-designed software running on a microcomputer interfaced with a National Instruments data acquisition board (NI-DAQ). To disrupt any remaining intact membranes, the fibre was submerged into a relaxing solution containing 0.5% Brij 58 for 30 s after which the fibre bath was exchanged twice with relaxing solution.

The experimental chamber was mounted on the stage of an inverted microscope. Sarcomere length was adjusted to 2.5 μm using an eyepiece micrometer (800×), and the length of the fibre (FL) was recorded. A digital photo (Pro IDEO CVC-140 camera) was taken of the fibre while it was briefly suspended in air. Fibre diameter was determined at three points along the length of the fibre using Scion Image software, and fibre CSA calculated from the mean diameter measurement, assuming the fibre forms a circular cross section when suspended in air (Metzger & Moss, 1987).

Experimental procedures

Fibres exhibiting non-uniform sarcomere lengths or regions of tearing were not studied (Moss, 1979). Additionally, data for a given fibre were not included if peak isometric force (P_0) declined by >15% or fibre compliance (determined from the *y*-axis intercept of slack test) exceeded 10% (Trappe *et al*. 2004). For most fibres, P_0 declined <10% from the beginning to the end of the experiment. Contractile function of individual fast type II and slow type I fibres was determined exactly as described previously for our 17-day microgravity study (Widrick *et al*. 1999). Briefly, the fibre was maximally activated in pCa 4.5 solution, allowed to reach peak isometric force (P_0), and slacked to a predetermined length, which caused tension to drop to zero. The time it took the fibre to take up the slack and initiate the redevelopment of tension was measured. The fibre was then returned to relaxing solution (15°C) and re-extended to its original fibre length. Each fibre was subjected to five different slack steps and fibre V_0 (FL s^{-1}) determined from the slope of the least squares regression line of the plot of slack distance *versus* the time

Journal of Physiology, Vol. 588, No. 18 (September 2010): pg. 3567-3592. DOI.

required for the redevelopment of force. Slack length changes never exceeded 20% of fibre length.

The rate constant of tension redevelopment (k_{tr}) was determined using the slack–unslack procedure (Metzger & Moss, 1990). To prevent sarcomere non-uniformity during tension redevelopment, Metzger & Moss (1990) used a laser to clamp the sarcomeres at 2.5 μm. The clamp procedure is time consuming and not practical when hundreds of fibres are studied. In preliminary studies, we determined that the k_{tr} of the slow type I fibre was identical with and without a laser clamp, while the fast type II fibre showed a significantly lower k_{tr} in the absence of a laser clamp (Fitzsimons *et al*. 2001). Thus, we determined the k_{tr} in slow but not fast fibres. The measurement requires activation of the fibre in pCa 4.5 and following attainment of steady tension a 400 μm slack, a 40 ms delay, and then re-extension to the original FL. Re-extension dissociates the cross-bridges, and tension redevelopment was best fitted with a first-order exponential equation where the rate constant k is k_{tr} and thought to reflect the rate limiting step in the generation of the high force state (Metzger & Moss, 1990).

Following the determination of V_0 and k_{tr}, isotonic load clamps were employed to measure force–velocity–power parameters. For each fibre, the force (as a percentage of peak force) and the corresponding shortening velocity for 15 force–velocity data points were fitted to the Hill equation with the use of an iterative non-linear curve-fitting procedure (Marquardt–Levenberg algorithm), and maximal shortening velocity (V_{max}) and the a/P_0 ratio determined (Widrick *et al*. 1998). Peak fibre power was calculated with the fitted parameters of the force–velocity curve and P_0 (Widrick *et al*. 1998). Composite force–velocity and force–power curves were constructed by summating velocities or power values from 0 to 100% of P_0 in increments of 1%.

In a subset of fibres (see Table 11 for the n for each fibre type), force–pCa relationships were determined by activating the fibres in a series of solutions with calcium concentrations ranging from pCa 6.8 to 4.5 exactly as described previously (Widrick *et al*. 1999). Hill plots were fitted to the data and the activation threshold, the one-half maximal activation (pCa_{50}), and slope of the force–calcium relationship below (n_2) and above (n_1) pCa_{50} determined (Widrick *et al*. 1999).

Journal of Physiology, Vol. 588, No. 18 (September 2010): pg. 3567-3592. DOI.

Fibre stiffness or the elastic modulus (E_0) was measured by oscillating the position motor at 1.5 kHz at an amplitude of 0.05% of FL both before (relaxing solution pCa 9.0), and during the measurement of peak force at the various pCa values. The elastic modulus E_0 at each pCa was calculated from the equation E_0 = (Δforce in activating solution −Δforce in relaxing solution/Δlength) (fibre length/fibre cross-sectional area).

Table 11. Force–pCa relationship in slow type I and fast type II fibres pre- and post-spaceflight

	SOL Type I		GM Type I		Type II	
Variable	Pre-flight	Post-flight	Pre-flight	Post-flight	Pre-flight	Post-flight
n	125	98	76	80	31	49
Activation threshold	6.96 ± 0.02	6.94 ± 0.03	6.85 ± 0.03	6.90 ± 0.03	6.63 ± 0.05	6.56 ± 0.03
pCa50	5.94 ± 0.02	6.00 ± 0.02*	5.86 ± 0.02	5.97 ± 0.03*	6.10 ± 0.04	6.09 ± 0.03
n_1	1.60 ± 0.05	1.72 ± 0.06	1.73 ± 0.07	1.89 ± 0.09	1.76 ± 0.20	2.14 ± 0.15
n_2	2.35 ± 0.04	2.72 ± 0.07*	2.43 ± 0.06	2.79 ± 0.09*	5.04 ± 0.38	5.49 ± 0.34

Values are means ± S.E.M.; *n*, no. of fibres studied; all values are pCa or –log of the Ca^{2+} concentration and pCa_{50}, –log of the Ca^{2+} concentration at half-maximal activation; n_1 and n_2, slope of Hill plot for values greater than and less than half-maximal activation, respectively. The type II data are composite means for all fast fibres from soleus and gastrocnemius muscles. *Significantly different from pre-flight value, $P < 0.05$.

SDS gel analysis of actin and myosin composition

After the contractile tests, the fibre was removed from the experimental set-up and solubilized in 10 μl of sodium dodecyl sulfate (SDS) sample buffer (6 mg ml^{-1} EDTA, 0.06 m tris(hydroxymethyl)aminomethane, 1% SDS, 2 mg ml^{-1} Bromophenol Blue, 15% glycerol, 5%β-mercaptoethanol), and stored at −80°C. Fibre types were identified by the myosin heavy chain (MHC) isoform pattern using 5% polyacrylamide gels as slow type I or fast type II. Fibres containing both slow and fast myosin (hybrid fibres) were not included in the analysis. Myosin (heavy and light chains), actin, tropomyosin and troponin profiles were determined by 12% polyacrylamide gel analysis (Widrick *et al*. 1997). For type I fibres, a computer-based image analysis system and software (LabWorks; UVP Inc., Upland, CA, USA) were used to quantify the relative density of the MHC and actin bands on the 12% gels. For Fig. 14*B*, actin/myosin ratio (actin band intensity/slow myosin band intensity) was plotted *versus* thin filament number per square micrometre for subjects A, C, D, E, F, G, H and I. For each subject, the actin/myosin ratio was determined on an average of 26 ± 4 (pre-flight) and 30 ± 6 (post-

Journal of Physiology, Vol. 588, No. 18 (September 2010): pg. 3567-3592. DOI.

flight) fibres, and the thin filament density on five pre- and five post-flight fibres using electron microscopy.

Figure 14. Correlations of fibre V_0 and actin content with thin filament density

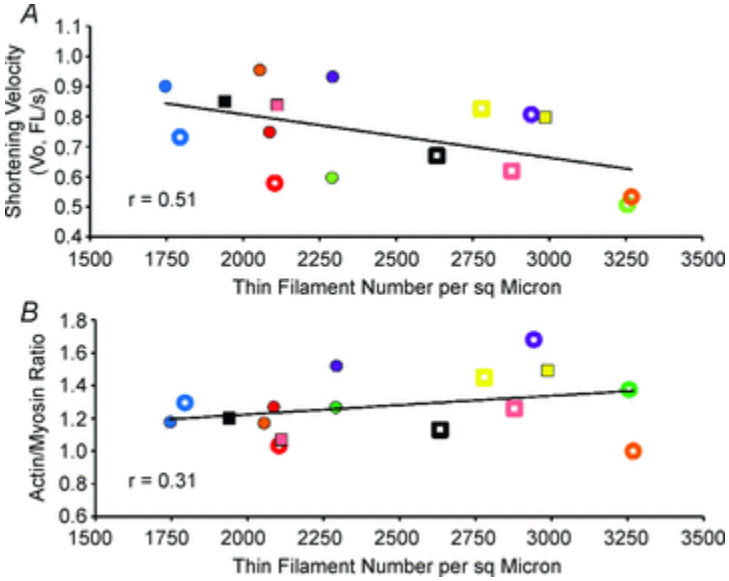

In pre- and post-flight soleus muscles, the shortening velocity (V_0) of type I fibres is low when thin filament density is high and the correlation is significant at $P < 0.05$ (*A*), while the actin/myosin ratio of type I fibres did not change pre- to post-flight and the correlation with thin filament density was not significant (*B*). Each subject is colour coded as shown in Fig. 1 with the filled symbols pre-flight and the partially filled post-flight.

Analysis of thin filament density by electron microscopy

Our previous studies demonstrated that in normal rat and human soleus muscle fibres, thin filaments varied in length, and during 17-day spaceflight and bedrest, the percentages of short thin filaments increased (Riley *et al*. 1998, 2000, 2005). In cross-sectioned sarcomeres, thin filament density was highest in the I band and fell off in the A band because the short filaments arising from the Z line were not long enough to reach the A band in a sarcomere at 2.5 μm length. For the present 180-day spaceflight muscles, a qualitative inspection of thin filament numbers in the I band near the Z line and within the A band (overlap A) where thin filaments first overlap thick filaments indicated that thin filaments were not missing as expected from 17 day flight data but appeared more abundant, pointing to increased thin filament length. Further into the A band nearer the M line, thin

Journal of Physiology, Vol. 588, No. 18 (September 2010): pg. 3567-3592. DOI.

filament number decreased, which made sense because only the longest thin filaments (~1.27 nm) could reach this far. Thus, to detect increased thin filament density due to increased thin filament length, thin filament densities were quantified near the M line in cross sections of sarcomeres of slow muscle fibres in the pre- and post-flight biopsy bundles from the solei of each subject. The concepts of thin filament length, thin filament density and location of near the M line measurement site are illustrated diagrammatically in Fig. 16.

Figure 16. Conceptual diagram of increasing thin filament density following prolonged spaceflight

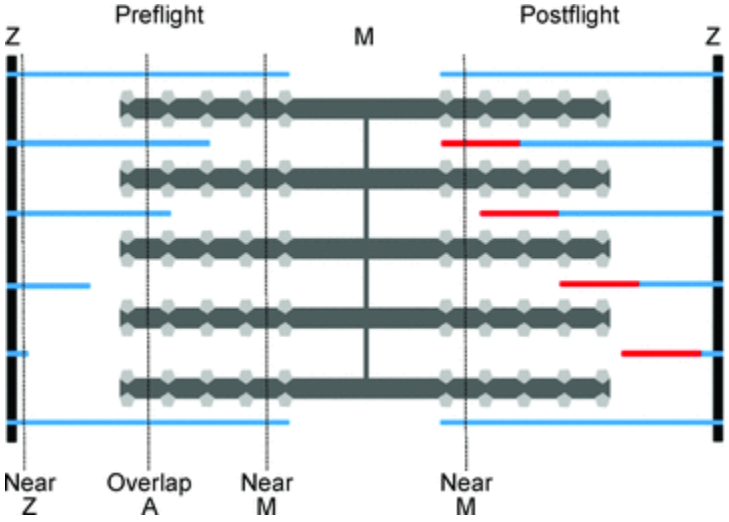

The sarcomere at 2.5 μm illustrates thin filament (blue line) density and lengths in a pre-flight muscle (left half) and post-flight density and lengths in the right half. Thin filaments arise from nucleation sites in the Z band and exhibit different lengths in normal skeletal muscles. The density of thin filaments is highest near the Z band (6 filaments in the Near Z region) and progressively decreases away from the Z band because some filaments are too short to overlap the A band (4 in Overlap A) and others end before reaching the Near M band region. After prolonged spaceflight, thin filament length increases (indicated by red extensions of thin filaments) and density increases in the Near M region (post-flight).

Cross sections (70 nm) of the epoxy-embedded muscle bundles were cut, contrasted with uranyl acetate and lead citrate and examined and imaged in a JEOL 100 CXII electron microscope (EM). The near M line regions of thick and thin filaments of slow fibres were imaged, and the EM negatives were scanned for computerized morphometrical analysis using MetaMorph 5.2 software. As conducted previously to achieve adequate statistical power, five slow fibres were sampled per soleus muscle per time point for a total of 90 fibres (Riley

Journal of Physiology, Vol. 588, No. 18 (September 2010): pg. 3567-3592. DOI.

et al. 2000, 2005). Group averages are reported as the mean ± s.e.m. The sarcomere length varied in the aldehyde fixed fibres, and it is known that myofilament density is directly related to sarcomere length (Riley *et al*. 2000, 2005). To normalize for sarcomere length differences among fibres, thick filament spacing was adjusted to 31.3 nm (2.5 μm sarcomere length). After normalization, the average thick filament density of the pre-flight fibres (999 ± 21 filaments μm^{-2}) was comparable (P = 0.07) to that of the post-flight fibres (945 ± 19μm^2), confirming standardization. Measurement of thick and thin filament densities was accomplished by counting the numbers of each filament type in a 0.0056 μm^2 grid square at ×201,000 magnification on the computer screen using Gunderson's rules for sampling (Riley *et al*. 2000, 2005). For non-biased sampling of thick and thin filament counts, the grid squares were positioned at random over the A band regions of thick and thin filament overlap within an estimated 100–300 nm of the M band in central myofibrils (Riley *et al*. 2002). The position of the sampling square was fine adjusted to insure that the corralled thick and thin filaments appears as dots, indicating cross section orientation.

Statistical analysis

To minimize operator bias, the morphological and physiological measurements were completed independently before the data were assembled for each subject to assess structural and functional correlations. For the functional studies, the fibres studied for each crew member for a given parameter were aggregated to obtain pre- and post-flight means. These data were analysed using a one-way ANOVA with Tukey's *post hoc* test. Group pre- and post-flight means (high *versus* low treadmill, and all crew members combined) were analysed with Student's *t* test for unpaired data. For morphological quantification, the pre- and post-flight group means were compared by subject paired *t* test. The thin filament densities of post-flight soleus fibres were compared with the control pre-flight fibres for each crew member using a two-tailed, unpaired *t* test analysis of five slow fibres per time point. When correlating thin filament density with V_0, the individual means of thin filament densities for the pre- and post-flight samples were compared with the V_0 means for slow fibres isolated

Journal of Physiology, Vol. 588, No. 18 (September 2010): pg. 3567-3592. DOI.

from the same biopsies. Statistical significance was accepted at $P < 0.05$. All data are presented as means ± s.e.m.

Results

For the determination of soleus fibre diameter, peak force (P_0), and maximal unloaded shortening velocity (V_0), 600 pre-flight (540 type I and 60 type II, a type I/type II ratio of 90%), and 542 post-flight (458 type I and 84 type II, a type I/type II ratio of 85%) fibres were analysed. For these same parameters, the gastrocnemius analysis included the study of 433 pre-flight (305 type I and 128 type II, a type I/type II ratio of 70%), and 325 post-flight (186 type I and 139 type II, a type I/type II ratio of 57%) fibres. The force–velocity and the force–pCa relationships were determined on fewer fibres, as following the V_0 determination one but not both of these relationships was determined. The main findings are described in the following paragraphs.

Fibre atrophy and peak force

Pre- and post-flight diameters and CSA for the slow type I fibres of the soleus and gastrocnemius are shown in Table 2 and peak force (mN and kN m^{-2}) in Tables 3 (soleus) and and44 (gastrocnemius). Corresponding fast fibre data are shown in Tables 5 and and6.6. In all but the fast gastrocnemius fibres, prolonged space flight elicited significant atrophy (as determined from fibre diameter and CSA) and decline in peak force (mN) with the degree of change soleus type I > soleus type II > gastrocnemius type I fibres. Considerable variability between crew members existed in both the degree of fibre atrophy and the loss of peak force (Tables 2–4). For example, crew member B showed no soleus type I fibre atrophy, and only a modest 10% loss in fibre force, whereas for crew member F, soleus type I fibre size and force were reduced by 51 and 70%, respectively (Tables 2 and and3).3). The decline in peak force was primarily caused by fibre atrophy as the crew average for soleus fibre force expressed in kN m^{-2} was not altered pre- *versus* post-flight, while absolute force in mN declined by 35% (Table 3). For crew members A and F, soleus fibre atrophy must have exceeded the contractile filament loss as fibre force per CSA significantly increased (Table 3). For the gastrocnemius

Journal of Physiology, Vol. 588, No. 18 (September 2010): pg. 3567-3592. DOI.

muscle, none of the crew members showed a significant decrease in type I fibre force expressed as kN m^{-2}, while all but subject I showed declines in absolute force that exceeded 18% (Table 4).

Table 2. Diameter and cross sectional area of the soleus and gastrocnemius slow type I fibre pre- and post-flight

		Sol Type I					Gastrocnemius Type I			
		Diameter		CSA			Diameter		CSA	
Crew member	*n*	(μm)	(%)	(μm^2)	(%)	*n*	(μm)	(%)	(μm^2)	(%)
A										
Pre-flight	70	107 ± 2		9277 ± 416		56	72 ± 2		4150 ± 186	
Post-flight	45	58 ± 1*	54	2663 ± 74*	28	39	58 ± 1*	81	2682 ± 97*	65
B										
Pre-flight	39	71 ± 2		4002 ± 193						
Post-flight	29	75 ± 2	106	4461 ± 204	111					
C										
Pre-flight	48	105 ± 2		8722 ± 316		10	99 ± 3		7802 ± 443	
Post-flight	47	83 ± 1*	79	5535 ± 183*	63	14	90 ± 5	91	6597 ± 741	85
D										
Pre-flight	52	99 ± 1		7817 ± 223		32	98 ± 2		7627 ± 396	
Post-flight	49	78 ± 2*	79	4822 ± 196*	62	24	74 ± 2*	76	4301 ± 195*	56
E										
Pre-flight	45	102 ± 3		8358 ± 473		32	100 ± 4		8185 ± 574	
Post-flight	64	87 ± 1*	85	6045 ± 164*	72	32	88 ± 1*	88	6060 ± 170*	74
F										
Pre-flight	41	121 ± 3		11756 ± 513		53	85 ± 2		5830 ± 245	
Post-flight	28	59 ± 1*	49	2798 ± 120*	24	13	69 ± 2*	81	3732 ± 161*	64
G										
Pre-flight	55	97 ± 1		7391 ± 176		44	78 ± 1		4807 ± 118	
Post-flight	56	85 ± 1*	88	5756 ± 208*	78	27	67 ± 2*	86	3556 ± 157*	74
H										
Pre-flight	104	89 ± 1		6316 ± 131		42	80 ± 1		5027 ± 160	
Post-flight	71	77 ± 1*	87	4676 ± 118*	74	13	68 ± 2*	85	3694 ± 221*	73
I										
Pre-flight	86	97 ± 1		7522 ± 184		36	65 ± 2		3381 ± 199	
Post-flight	69	91 ± 2*	94	6661 ± 231*	89	24	63 ± 1	97	3177 ± 88	94
High treadmill										
Pre-flight	243	90 ± 1		6517 ± 936		118	85 ± 1		6006 ± 1091	
Post-flight	220	82 ± 1*	92 ± 5	5235 ± 391	84 ± 9	72	76 ± 1*	86 ± 1	4437 ± 813	74 ± 0
Low Treadmill										
Pre-flight	297	104 ± 1		9019 ± 753		187	80 ± 1		5758 ± 892	
Post-flight	238	77 ± 1*	71 ± 9	4496 ± 778*	53 ± 12	114	68 ± 1*	85 ± 4	4098 ± 681	73 ± 7
All crew members										
Pre-flight	540	98 ± 1		7907 ± 705		305	82 ± 1		5851 ± 643	
Post-flight	458	79 ± 1*	80 ± 6	4824 ± 459*	67 ± 9	186	71 ± 1*	86 ± 2	4225 ± 490†	76 ± 5

High treadmill group subjects B, E, G and H, and low treadmill group subjects A, C, D, F and I; values are means ± S.E.M.; *n*, no. of fibres studied. P_0, peak isometric force; %, percentage of pre-flight value; V_0, maximal shortening velocity; FL, fibre length. *Significantly different from pre-flight value, $P < 0.05$.

Journal of Physiology, Vol. 588, No. 18 (September 2010): pg. 3567-3592. DOI.

Table 3. Peak force and maximal shortening velocity of the soleus slow type I fibre pre- and post-flight

		P_o			V_o	
Crew member	*n*	(mN)	(%)	(kN m^{-2})	(FL s^{-1})	(%)
A						
Pre-flight	70	0.86 ± 0.04		97 ± 2	0.90 ± 0.04	
Post-flight	45	0.38 ± 0.01*	44	144 ± 4*	0.73 ± 0.04*	81
B						
Pre-flight	39	0.48 ± 0.02		124 ± 4	1.13 ± 0.16	
Post-flight	29	0.43 ± 0.02	90	97 ± 3*	0.80 ± 0.03	71
C						
Pre-flight	48	0.97 ± 0.04		113 ± 3	0.60 ± 0.02	
Post-flight	47	0.55 ± 0.02*	57	102 ± 4	0.51 ± 0.03*	85
D						
Pre-flight	52	0.96 ± 0.03		123 ± 3	0.93 ± 0.05	
Post-flight	49	0.55 ± 0.02*	57	116 ± 3	0.81 ± 0.04	87
E						
Pre-flight	45	0.78 ± 0.03		97 ± 3	0.80 ± 0.05	
Post-flight	64	0.66 ± 0.02*	85	111 ± 2*	0.83 ± 0.04	104
F						
Pre-flight	41	1.29 ± 0.05		114 ± 4	0.96 ± 0.06	
Post-flight	28	0.39 ± 0.01*	30	143 ± 4*	0.53 ± 0.03*	56
G						
Pre-flight	55	0.86 ± 0.03		118 ± 4	0.85 ± 0.04	
Post-flight	56	0.63 ± 0.03*	73	109 ± 3^{+}	0.67 ± 0.03*	79
H						
Pre-flight	104	0.74 ± 0.02		118 ± 2	0.84 ± 0.03	
Post-flight	71	0.47 ± 0.02*	64	104 ± 4*	0.62 ± 0.02*	74
I						
Pre-flight	86	0.91 ± 0.02		124 ± 3	0.75 ± 0.03	
Post-flight	69	0.74 ± 0.03*	81	113 ± 3*	0.58 ± 0.03*	77
High treadmill						
Pre-flight	243	0.73 ± 0.01		115 ± 2	0.88 ± 0.03	
Post-flight	220	0.56 ± 0.01*	77	106 ± 2*	0.72 ± 0.02*	81
Low treadmill						
Pre-flight	297	0.97 ± 0.02		114 ± 1	0.83 ± 0.02	
Post-flight	238	0.56 ± 0.01*	58	121 ± 2*	0.64 ± 0.02*	77
All crew members						
Pre-flight	540	0.86 ± 0.01		115 ± 1	0.85 ± 0.02	
Post-flight	458	0.56 ± 0.01*	65	114 ± 1	0.68 ± 0.01*	80

High treadmill group subjects B, E, G and H, and low treadmill group subjects A, C, D, F and I; values are means ± S.E.M.; *n*, no. of fibres studied. P_0, peak isometric force; %, percentage of pre-flight value; V_0, maximal shortening velocity; FL, fibre length. *Significantly different from pre-flight value, $P < 0.05$. For subject C the *n* for V_o was 35 and 31 for the pre- and post-flight sample.

Journal of Physiology, Vol. 588, No. 18 (September 2010): pg. 3567-3592. DOI.

Table 4. Peak force and maximal shortening velocity of the gastrocnemius slow type I fibre pre- and post-flight

		P_o			V_o	
Crew member	*n*	(mN)	(%)	(kN m^{-2})	(FL s^{-1})	(%)
A						
Pre-flight	56	0.47 ± 0.02		116 ± 3	0.86 ± 0.04	
Post-flight	39	0.38 ± 0.01*	81	144 ± 4*	0.71 ± 0.05*	82
C						
Pre-flight	10	0.78 ± 0.05		100 ± 3	0.67 ± 0.03	
Post-flight	14	0.59 ± 0.05*	76	92 ± 5	0.59 ± 0.03	89
D						
Pre-flight	32	0.83 ± 0.03		113 ± 3	0.95 ± 0.06	
Post-flight	24	0.46 ± 0.02*	55	118 ± 4	0.85 ± 0.05	90
E						
Pre-flight	32	0.82 ± 0.04		107 ± 5	1.05 ± 0.06	
Post-flight	32	0.67 ± 0.02*	82	112 ± 4	0.91 ± 0.07	87
F						
Pre-flight	53	0.73 ± 0.08		136 ± 20	0.83 ± 0.05	
Post-flight	13	0.45 ± 0.09	62	121 ± 5	0.65 ± 0.06	78
G						
Pre-flight	44	0.53 ± 0.01		114 ± 4	0.80 ± 0.05	
Post-flight	27	0.35 ± 0.02*	66	103 ± 9	0.59 ± 0.04*	74
H						
Pre-flight	42	0.56 ± 0.01		114 ± 3	0.87 ± 0.04	
Post-flight	13	0.43 ± 0.04*	77	118 ± 10	0.58 ± 0.04*	70
I						
Pre-flight	36	0.37 ± 0.02		120 ± 8	0.80 ± 0.04	
Post-flight	24	0.39 ± 0.02	105	125 ± 5	0.67 ± 0.04*	84
High treadmill						
Pre-flight	118	0.62 ± 0.02		112 ± 2	0.89 ± 0.03	
Post-flight	72	0.50 ± 0.02*	81	109 ± 4	0.73 ± 0.04*	82
Low treadmill						
Pre-flight	187	0.60 ± 0.03		121 ± 6	0.85 ± 0.02	
Post-flight	114	0.43 ± 0.01*	72	125 ± 3	0.71 ± 0.02*	84
All crew members						
Pre-flight	305	0.61 ± 0.02		118 ± 4	0.86 ± 0.02	
Post-flight	186	0.46 ± 0.01*	75	119 ± 2	0.72 ± 0.02*	83

High treadmill group subjects B, E, G and H, and low treadmill group subjects A, C, D, F and I; values are means ± S.E.M.; *n*, no. of fibres studied. P_0, peak isometric force; %, percentage of pre-flight value; V_0, maximal shortening velocity; FL, fibre length. *Significantly different from pre-flight value, $P < 0.05$.

Journal of Physiology, Vol. 588, No. 18 (September 2010): pg. 3567-3592. DOI.

Table 5. Diameter, cross sectional area, peak force, and maximal shortening velocity of the soleus fast type II fibre pre- and post-flight

		Diameter		CSA		P_o			V_o	
Condition	*n*	(μm)	(%)	(μm^2)	(%)	(mN)	(%)	(kN m^{-2})	(FL s^{-1})	(%)
High treadmill										
Pre-flight	37	90 ± 2		6548 ± 296		0.82 ± 0.04		129 ± 3	2.62 ± 0.20	
Post-flight	24	87 ± 3	97	6170 ± 490	94	0.80 ± 0.07	98	130 ± 6	2.52 ± 0.26	96
Low treadmill										
Pre-flight	23	105 ± 5		9054 ± 845		1.20 ± 0.09		139 ± 5	2.74 ± 0.25	
Post-flight	60	77 ± 2*	73	4818 ± 296*	53	0.68 ± 0.03*	57	144 ± 3	3.10 ± 0.17	113
All crew members										
Pre-flight	60	95 ± 2		7358 ± 396		0.97 ± 0.05		133 ± 2	2.66 ± 0.16	
Post-flight	84	80 ± 2*	84	5245 ± 255*	71	0.71 ± 0.03*	73	140 ± 3	2.94 ± 0.15	111

High treadmill group subjects B, E, G and H, and low treadmill group subjects A, C, D, F and I; values are means ± S.E.M.; *n*, no. of fibres studied. P_0, peak isometric force; %, percentage of pre-flight value; V_0, maximal shortening velocity; FL, fibre length. *Significantly different from pre-flight value, $P < 0.05$.

Table 6. Diameter, cross sectional area, peak force, and maximal shortening velocity of the gastrocnemius fast type II fibre pre- and post-flight

		Diameter		CSA		P_o			V_o	
Condition	*n*	(μm)	(%)	(μm^2)	(%)	(mN)	(%)	(kN m^{-2})	(FL s^{-1})	(%)
High treadmill										
Pre-flight	52	91 ± 2		9709 ± 361		0.97 ± 0.05		147 ± 3	3.45 ± 0.17	
Post-flight	58	85 ± 2	93	5845 ± 221*	87	0.78 ± 0.03*	80	136 ± 3	2.78 ± 0.13*	81
Low treadmill										
Pre-flight	76	69 ± 2		3970 ± 223		0.57 ± 0.03		153 ± 4	3.30 ± 0.14	
Post-flight	81	70 ± 1	101	4012 ± 168	101	0.61 ± 0.03	107	154 ± 3	2.76 ± 0.13*	84
All crew members										
Pre-flight	128	78 ± 2		5045 ± 282		0.73 ± 0.03		151 ± 3	3.36 ± 0.11	
Post-flight	139	77 ± 1	99	4774 ± 154	95	0.68 ± 0.02	93	147 ± 2	2.77 ± 0.09*	82

High treadmill group subjects B, E, G and H, and low treadmill group subjects A, C, D, F and I; values are means ± S.E.M.; *n*, no. of fibres studied. P_0, peak isometric force; %, percentage of pre-flight value; V_0, maximal shortening velocity; FL, fibre length. *Significantly different from pre-flight value, $P < 0.05$.

The percentage change (pre- to post-flight) in the mean soleus type I fibre diameter for each crew member showed a significant correlation with the percentage change in the pre- to post-flight soleus muscle volume determined by MRI (Fig. 1). The mean space flight-induced decline in soleus type I fibre CSA was 33%, a value that agrees well with CSA determinations made on histochemically stained muscle fibre bundles (Fig. 2). In the soleus, the extent of type I fibre atrophy tended to be associated with an increase in the number of fast type II fibres post-flight. Thus, crew members with the highest percentage decline in mean fibre diameter showed the greatest increase in the number of fast type II fibres (Fig. 3).

Journal of Physiology, Vol. 588, No. 18 (September 2010): pg. 3567-3592. DOI.

Figure 1. Relationship between soleus fibre atrophy and the decline in whole muscle volume with prolonged space flight

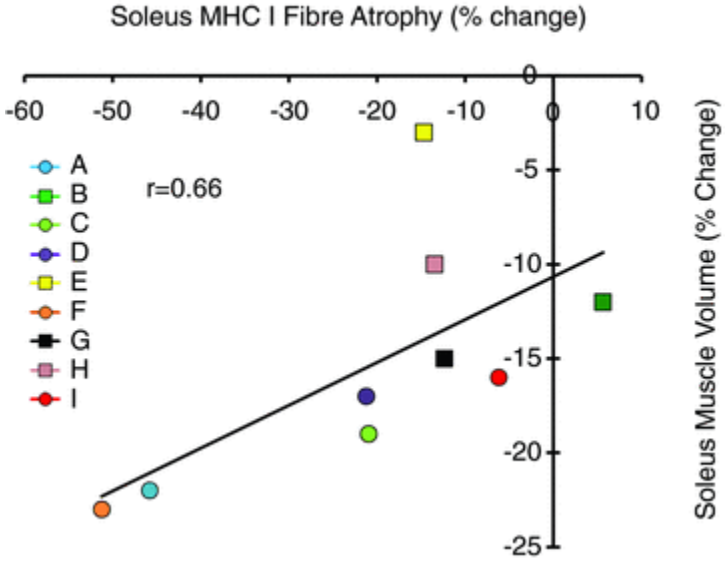

The percentage change (pre- to post-flight) in the mean type I fibre diameter is plotted *versus* the percentage change in soleus muscle volume for each crew member. The crew members A–I are identified by a specific colour with the low and high treadmill users indicated by circles and squares, respectively. The variables showed a significant ($P < 0.05$) correlation with an $r = 0.66$.

Figure 2. Representative pre- and post-flight fibre bundle

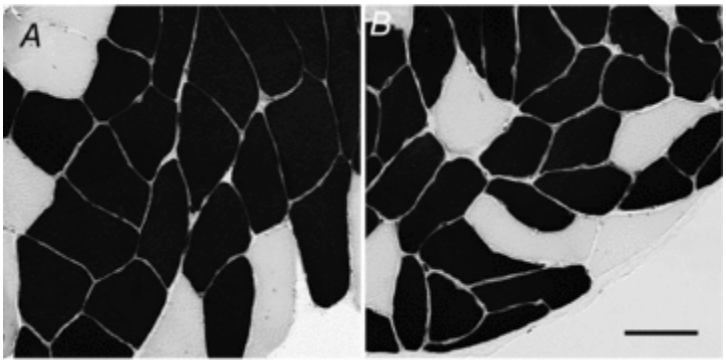

Cryostat cross sections of subject C pre-flight (*A*) and post-flight (*B*) soleus muscle fibres were stained histochemically for actomyosin ATPase activity after acid preincubation (method of Huckstorf *et al*. 2000). Slow fibres are darkly reactive, and fast fibres are lightly reactive. Based on computerized digitizing planimetry, the post-flight slow fibres are 31.5% smaller in cross-sectional area. Bar equals 75 μm for both panels.

Journal of Physiology, Vol. 588, No. 18 (September 2010): pg. 3567-3592. DOI.

Figure 3. Relationship between microgravity induced fibre atrophy and percentage increase in fast fibres in slow soleus muscle

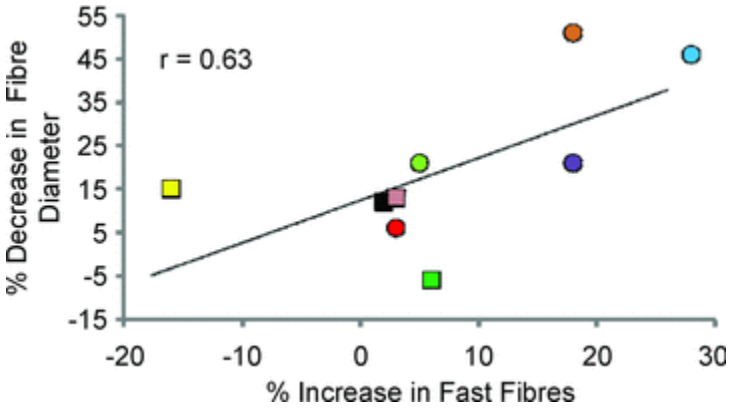

Symbols plot the percentage decrease in mean fibre diameter *versus* the percentage increase in fast fibre type for each crew member. Each subject A–I is colour coded as in Fig. 1.

The volume of treadmill use appeared to influence the muscle atrophy response while on the ISS for 6 months. As a result, we subdivided the crew members into those running 200 min week^{-1} or more (high treadmill) from those running less than 100 min week^{-1} (low treadmill). The weekly treadmill running average for each crew member has been published elsewhere (Trappe *et al*. 2009). The high treadmill group showed significantly less space flight-induced atrophy and loss of force in the soleus slow type I and fast type II fibres (Tables 2, ,33 and and5),5), while for the gastrocnemius no differences between groups for these parameters was observed for type I (Tables 2 and and4)4) or type II (Table 6) fibres. The protective effect of the treadmill countermeasure for the soleus type I fibre is perhaps best appreciated by comparing the plot of fibre atrophy *versus* force pre- and post-flight for each crew member (Figs 4 and and5).5). The low treadmill group showed an average pre-flight force of ~100 mN and diameter of 100 μm while post-flight the relationship for force *versus* diameter was shifted down and to the left so that the majority of the fibres generated a peak force <100 mN and had a fibre diameter <100 μm (Fig. 4). In comparison, the down and left shift of the force *versus* diameter plot for the high treadmill group was less apparent (Fig. 5). The average weekly treadmill running showed a significant inverse correlation with the percentage of soleus type I fibre atrophy with r = 0.68 (Fig. 6). A second observation that seemed to impact the extent of fibre atrophy and hence the decline in force was

the pre-flight diameter. The larger the initial fibre diameter the greater the atrophy such that a significant inverse correlation (r = 0.87) was observed between the mean pre-flight soleus type I fibre diameter and the pre/post fibre diameter ratio expressed as a percentage (Fig. 6).

Figure 4. Relationship between fibre diameter (μm) and peak Ca^{2+} activated isometric force (mN) pre- and post-flight for low treadmill group

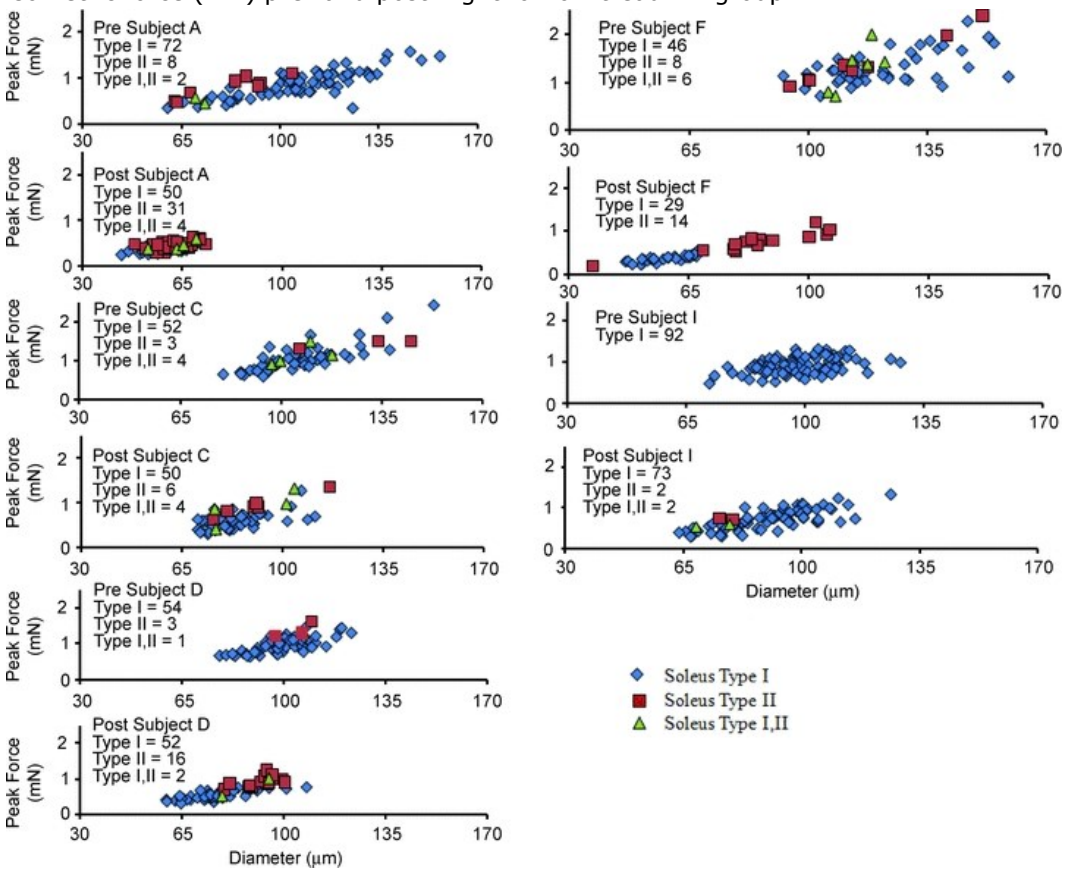

Each symbol represents the result of a single soleus fibre. Type I fibres, blue diamonds. Type II fibres, red squares. Hybrid Type I/II fibres, green triangles. Number of fibres for each fibre type and crew member are shown.

Journal of Physiology, Vol. 588, No. 18 (September 2010): pg. 3567-3592. DOI.

Figure 5. Relationship between fibre diameter (μm) and peak Ca^{2+} activated isometric force (mN) pre- and post-flight for high treadmill group

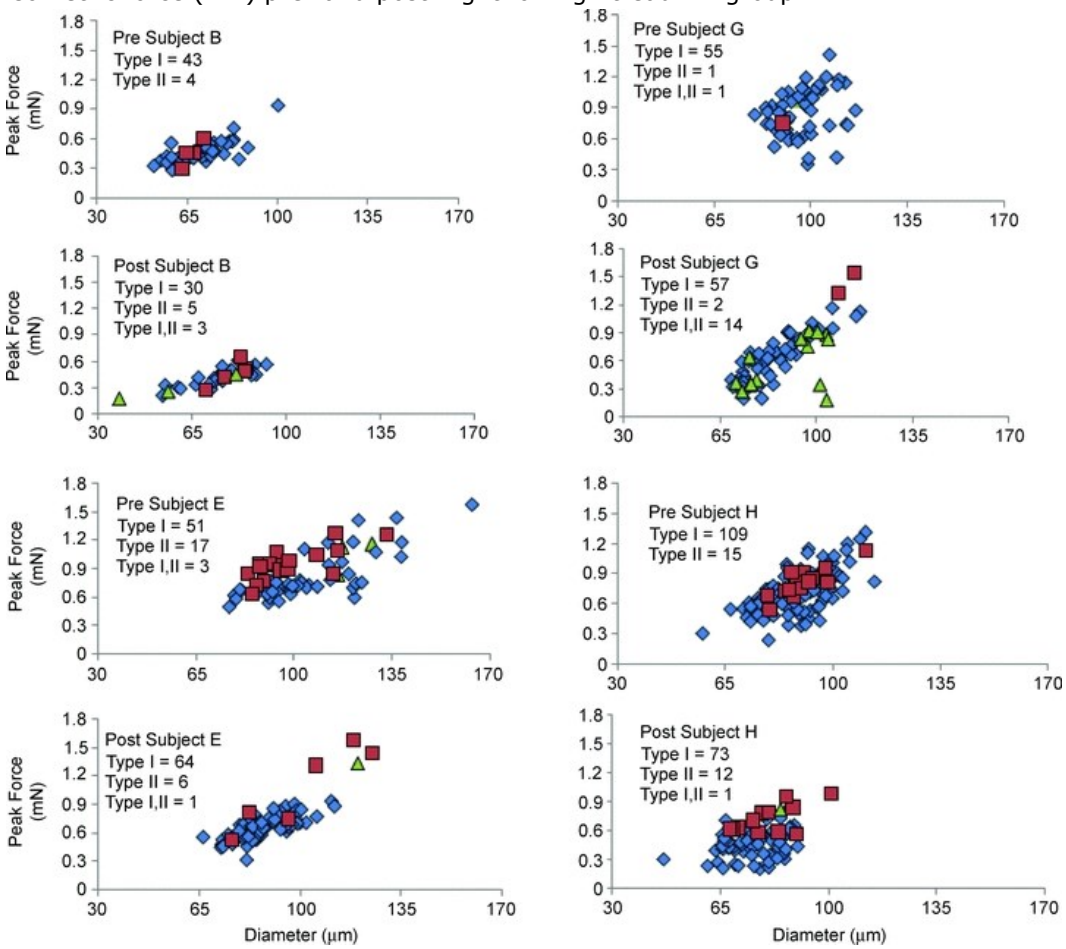

Each symbol represents the result of a single soleus fibre. Type I fibres, blue diamonds. Type II fibres, red squares. Hybrid Type I/II fibres, green triangles. Number of fibres for each fibre type and crew member are shown.

Journal of Physiology, Vol. 588, No. 18 (September 2010): pg. 3567-3592. DOI.

Figure 6. Correlation of soleus type I fibre atrophy with treadmill running and pre-flight fibre diameter

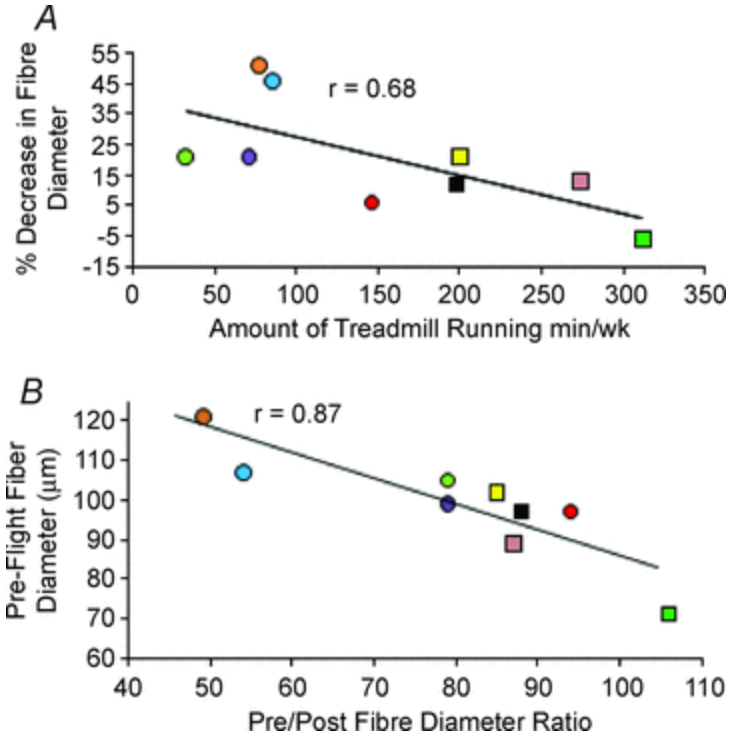

A, relationship between microgravity-induced fibre atrophy and amount of treadmill running (min week^{-1}). Symbols plot the percentage decrease in mean fibre diameter *versus* amount of treadmill running (min week^{-1}) for each crew member. *B*, relationship between pre-flight fibre diameter (µm) and percentage fibre atrophy. Symbols plot the mean pre-flight fibre diameter *versus* percentage fibre atrophy. For both the top and bottom plots, each subject is colour coded as shown in Fig. 1. The circles and squares indicate low and high treadmill groups, respectively.

Figure 7 plots the mean force (mN) *versus* diameter for each crew member pre- (circles) and post-flight (triangles) for fast type II fibres from the soleus and gastrocnemius. For the soleus, the plot was similar to that observed for the slow fibre type as post-flight the force to diameter relationship was shifted down (force loss) and to the left (diameter loss) in the low treadmill group with virtually no change in the plot (pre *versus* post) for the high treadmill group. In contrast, the gastrocnemius fast type II fibres were not protected by an increased amount of treadmill running (Fig. 7 and Table 6).

Journal of Physiology, Vol. 588, No. 18 (September 2010): pg. 3567-3592. DOI.

Figure 7. Relationship between fibre diameter (μm) and peak Ca^{2+} activated isometric force (mN) pre- and post-flight for type II fibres

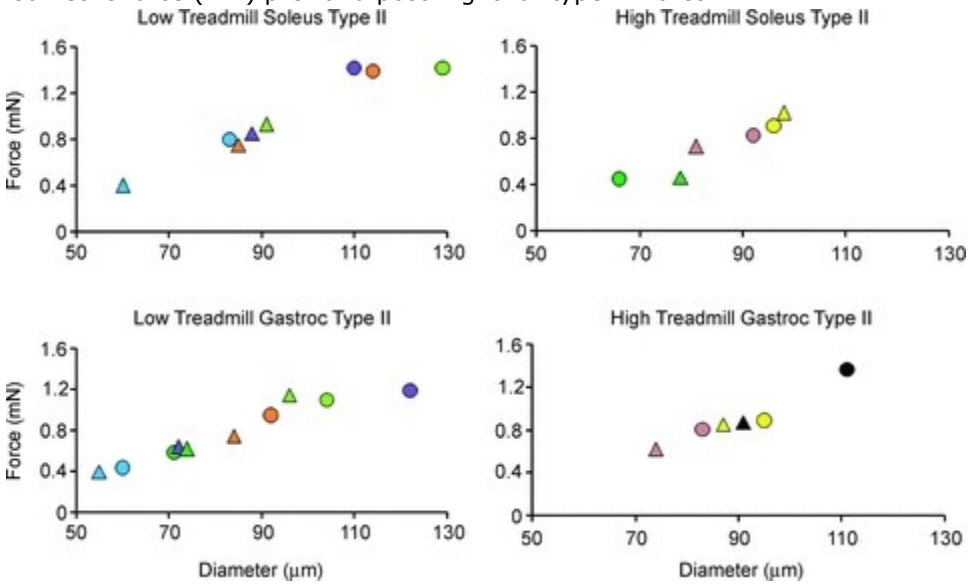

Each subject is colour coded as shown in Fig. 1. The average pre- and post-flight values are represented by circles and triangles, respectively. The plots show soleus type II fibres for the low (top left) and high (top right) treadmill groups, and gastrocnemius type II fibres from the low (bottom left) and high (bottom right) treadmill groups.

Maximal shortening velocity (V_0) and rate of tension development (k_{tr})

With the exception of the soleus fast type II fibres, which were unaltered by space flight (Table 5), the maximal unloaded shortening velocity (V_0) measured by the slack test declined by ~20% in both muscles and fibre types studied (Tables 3, ,44 and and6).6). Unlike fibre size and force, the decline in V_0 post-flight was not influenced by the extent of treadmill running. The rate constants of tension redevelopment (k_{tr}) in slow type I fibres of the soleus and gastrocnemius muscles were not significantly different and neither was altered by space flight (Table 7).

Journal of Physiology, Vol. 588, No. 18 (September 2010): pg. 3567-3592. DOI.

Table 7. Peak stiffness (E_0),P_0/E_0 ratio and the rate constant of tension redevelopment (k_{tr}) of the slow type I fibre pre- and post-spaceflight

Condition	E_0	P_0/E_0	k_{tr}
Sol Type I fibre			
Pre-flight	2.16 ± 0.07 (146)	62.6 ± 2.0	1.58 ± 0.04 (164)
Post-flight	2.47 ± 0.09 (103)*	52.3 ± 1.9*	1.55 ± 0.04 (127)
GM Type I fibre			
Pre-flight	2.22 ± 0.08 (90)	64.3 ± 2.2	1.47 ± 0.04 (111)
Post-flight	2.61 ± 0.12 (89)*	53.6 ± 2.4*	1.44 ± 0.03 (109)

Values are means ± S.E.M.; no. of fibres studied shown in parentheses; E_0, peak elastic modulus; P_0, peak isometric force; k_{tr}, rate constant of tension redevelopment. *Significantly different from pre-flight value, $P < 0.05$.

Fibre stiffness

Peak fibre stiffness (E_0), a property thought to reflect the number of attached cross-bridges, increased in the slow fibre type in both the soleus and gastrocnemius muscles (Table 7). The peak force (P_0)/peak stiffness (E_0) ratio was significantly less post-flight which suggests that if the higher stiffness was caused by more cross-bridges, the additional bridges were likely to be in a low force (weak binding) state.

V_{max}, peak power, and force and velocity at peak power

Similar to V_0 (the maximal unloaded shortening velocity measured by the slack test), the maximal shortening velocity derived from the Hill plot of the force–velocity relationship (V_{max}) was significantly depressed post-flight compared to pre-flight in the slow type I fibre from both the soleus and the gastrocnemius (Tables 8 and and9).9). Six of the nine and five of nine crew members showed a significant post-flight decline in type I fibre V_{max} in the soleus and gastrocnemius muscles, respectively (Tables 8 and and99).

Table 8. V_{max}, peak power, force and velocity at peak power for soleus slow type I fibre pre- and post-flight

Crew Member		V_{max}	a/P_0	Peak power			Force at PP	Vel at PP
	n	(FL s^{-1})		(μN FL s^{-1})	(%)	(W l^{-1})	(mN)	(FL s^{-1})
A								
Pre-flight	49	0.91 ± 0.05	0.036 ± 0.002	19.39 ± 1.39		2.04 ± 0.09	0.137 ± 0.006	0.139 ± 0.006
Post-flight	25	0.77 ± 0.05*	0.028 ± 0.002*	5.36 ± 0.29*	28	2.04 ± 0.08	0.052 ± 0.002*	0.103 ± 0.005*
B								
Pre-flight	19	0.88 ± 0.05	0.038 ± 0.002	10.37 ± 0.75		2.64 ± 0.13	0.075 ± 0.005	0.136 ± 0.004
Post-flight	11	0.76 ± 0.04	0.033 ± 0.002	7.35 ± 0.39*	71	1.60 ± 0.07*	0.064 ± 0.003	0.114 ± 0.005*
C								
Pre-flight	25	0.95 ± 0.06	0.029 ± 0.001	20.86 ± 2.61		2.31 ± 0.20	0.146 ± 0.009	0.134 ± 0.008
Post-flight	28	0.93 ± 0.07	0.033 ± 0.003	11.13 ± 0.84*	53	2.11 ± 0.16	0.084 ± 0.003*	0.129 ± 0.007
D								
Pre-flight	32	1.04 ± 0.05	0.024 ± 0.001	17.95 ± 1.10		2.26 ± 0.11	0.132 ± 0.004	0.133 ± 0.006
Post-flight	28	0.83 ± 0.05*	0.030 ± 0.002*	9.45 ± 0.68*	53	1.90 ± 0.09*	0.079 ± 0.003*	0.117 ± 0.006*
E								
Pre-flight	26	0.90 ± 0.07	0.026 ± 0.002	13.08 ± 1.19		1.43 ± 0.05	0.110 ± 0.007	0.117 ± 0.007
Post-flight	40	0.71 ± 0.03*	0.031 ± 0.002	9.45 ± 0.38*	72	1.59 ± 0.06	0.093 ± 0.003*	0.101 ± 0.003*
F								
Pre-flight	29	0.87 ± 0.06	0.025 ± 0.001	17.11 ± 0.83		1.50 ± 0.08	0.157 ± 0.007	0.113 ± 0.007
Post-flight	6	0.61 ± 0.09	0.051 ± 0.010*	7.00 ± 1.83*	41	2.70 ± 0.67*	0.061 ± 0.006*	0.110 ± 0.004
G								
Pre-flight	38	0.78 ± 0.04	0.024 ± 0.001	9.94 ± 0.64		1.35 ± 0.08	0.103 ± 0.005	0.100 ± 0.005
Post-flight	26	0.56 ± 0.03*	0.032 ± 0.002*	5.90 ± 0.50*	59	1.05 ± 0.05*	0.079 ± 0.008*	0.080 ± 0.003*
H								
Pre-flight	45	0.90 ± 0.05	0.025 ± 0.001	9.09 ± 0.34		1.55 ± 0.06	0.082 ± 0.004	0.117 ± 0.005
Post-flight	38	0.52 ± 0.03*	0.033 ± 0.002*	4.40 ± 0.28*	48	0.98 ± 0.07*	0.058 ± 0.003*	0.077 ± 0.004*
I								
Pre-flight	48	0.72 ± 0.03	0.024 ± 0.001	10.02 ± 0.45		1.34 ± 0.07	0.111 ± 0.005	0.091 ± 0.003
Post-flight	37	0.46 ± 0.02*	0.032 ± 0.001*	6.48 ± 0.48*	65	1.00 ± 0.06*	0.094 ± 0.005*	0.067 ± 0.003*
High Treadmill (4)								
Pre-flight	128	0.86 ± 0.03	0.027 ± 0.001	10.35 ± 0.57		1.63 ± 0.05	0.093 ± 0.003	0.115 ± 0.003
Post-flight	114	0.62 ± 0.02*	0.032 ± 0.001*	6.77 ± 0.28*	63 ± 6	1.26 ± 0.04*	0.076 ± 0.003*	0.089 ± 0.002*
Low Treadmill (5)								
Pre-flight	183	0.88 ± 0.02	0.028 ± 0.001	16.52 ± 0.64		1.84 ± 0.05	0.134 ± 0.003	0.121 ± 0.003
Post-flight	124	0.76 ± 0.04*	0.031 ± 0.001	7.98 ± 0.35*	48 ± 6	1.77 ± 0.07	0.077 ± 0.002*	0.104 ± 0.004*
All Crew								
Pre-flight	311	0.88 ± 0.02	0.027 ± 0.001	14.20 ± 0.45		1.76 ± 0.04	0.117 ± 0.002	0.119 ± 0.002
Post-flight	238	0.68 ± 0.02*	0.032 ± 0.001*	7.47 ± 0.24*	54 ± 5	1.53 ± 0.05*	0.077 ± 0.002*	0.097 ± 0.002*

High treadmill group subjects B, E, G and H, and low treadmill group subjects A, C, D, F and I; values are means ± S.E.M.; n, no. of fibres studied. V_{max}, maximal unloaded shortening velocity determined from the Hill plot; a/P_o, unitless parameter describing curvature of the force–velocity relationship. The relative power unit of watts per litre (W l^{-1}) is equivalent of kN m^{-2} FL s^{-1}; Vel at PP, velocity at peak power; Force at PP, force at peak power; FL, fibre length; no. of high and low treadmill crew members listed in parentheses. *Significantly different from pre-flight value, $P < 0.05$.

Table 9. V_{max}, peak power, force and velocity at peak power for gastrocnemius slow type I fibre pre- and post-flight

Crew member		V_{max}	a/P_0	Peak power			Force at PP	Vel at PP
	n	(FL s^{-1})		(μN FL s^{-1})	(%)	(W l^{-1})	(mN)	(FL s^{-1})
A								
Pre-flight	42	0.87 ± 0.04	0.036 ± 0.002	10.04 ± 0.59		2.34 ± 0.10	0.074 ± 0.003	0.133 ± 0.005
Post-flight	26	0.72 ± 0.06*	0.034 ± 0.003	5.64 ± 0.34*	56	2.15 ± 0.10	0.054 ± 0.002*	0.103 ± 0.006*
C								
Pre-flight	10	0.64 ± 0.03	0.038 ± 0.003	12.07 ± 0.86		1.56 ± 0.09	0.120 ± 0.009	0.100 ± 0.003
Post-flight	10	0.64 ± 0.04	0.032 ± 0.003	6.90 ± 0.44*	57	1.25 ± 0.06*	0.074 ± 0.006*	0.093 ± 0.004
D								
Pre-flight	28	0.86 ± 0.06	0.027 ± 0.001	13.48 ± 0.85		1.79 ± 0.09	0.115 ± 0.004	0.116 ± 0.005
Post-flight	24	0.78 ± 0.10	0.030 ± 0.002	7.24 ± 0.44*	54	1.71 ± 0.09	0.071 ± 0.004*	0.105 ± 0.008
E								
Pre-flight	24	1.08 ± 0.05	0.024 ± 0.001	16.21 ± 0.86		1.88 ± 0.13	0.117 ± 0.006	0.139 ± 0.005
Post-flight	26	0.69 ± 0.05*	0.032 ± 0.002*	8.85 ± 0.39*	55	1.47 ± 0.06*	0.091 ± 0.004*	0.099 ± 0.005*
F								
Pre-flight	40	0.75 ± 0.04	0.025 ± 0.001	7.37 ± 0.41		1.28 ± 0.05	0.079 ± 0.004	0.097 ± 0.005
Post-flight	12	0.69 ± 0.07	0.030 ± 0.003	5.70 ± 0.23*	77	1.50 ± 0.07*	0.061 ± 0.003*	0.094 ± 0.006
G								
Pre-flight	33	0.79 ± 0.04	0.022 ± 0.001	6.30 ± 0.28		1.32 ± 0.06	0.064 ± 0.002	0.100 ± 0.005
Post-flight	25	0.51 ± 0.04*	0.036 ± 0.005*	3.40 ± 0.27*	54	1.01 ± 0.09*	0.050 ± 0.005*	0.074 ± 0.004*
H								
Pre-flight	32	0.77 ± 0.04	0.027 ± 0.002	7.31 ± 0.36		1.42 ± 0.07	0.073 ± 0.003	0.101 ± 0.004
Post-flight	11	0.60 ± 0.07*	0.037 ± 0.005*	4.94 ± 0.44*	68	1.41 ± 0.16	0.058 ± 0.006*	0.087 ± 0.005*
I								
Pre-flight	29	0.82 ± 0.04	0.025 ± 0.001	4.69 ± 0.22		1.45 ± 0.11	0.045 ± 0.002	0.106 ± 0.004
Post-flight	24	0.52 ± 0.04*	0.034 ± 0.003*	4.11 ± 0.24	88	1.31 ± 0.08	0.056 ± 0.003*	0.073 ± 0.004*
High treadmill (3)								
Pre-flight	89	0.86 ± 0.03	0.024 ± 0.001	9.34 ± 0.53		1.51 ± 0.05	0.082 ± 0.003	0.111 ± 0.003
Post-flight	62	0.60 ± 0.03*	0.034 ± 0.002*	5.96 ± 0.38*	59 ± 5	1.27 ± 0.06*	0.069 ± 0.004*	0.087 ± 0.003*
Low treadmill (5)								
Pre-flight	149	0.81 ± 0.02	0.029 ± 0.001	9.07 ± 0.36		1.73 ± 0.05	0.081 ± 0.003	0.113 ± 0.003
Post-flight	96	0.67 ± 0.03*	0.032 ± 0.001	5.80 ± 0.20*	66 ± 7	1.66 ± 0.05	0.062 ± 0.002*	0.094 ± 0.003*
All crew								
Pre-flight	238	0.83 ± 0.02	0.027 ± 0.001	9.17 ± 0.30		1.64 ± 0.04	0.081 ± 0.002	0.112 ± 0.002
Post-flight	158	0.64 ± 0.02*	0.033 ± 0.001*	5.86 ± 0.19*	64 ± 5	1.51 ± 0.04	0.065 ± 0.002*	0.091 ± 0.002*

High treadmill group subjects B, E, G and H, and low treadmill group subjects A, C, D, F and I; values are means ± S.E.M.; n, no. of fibres studied. V_{max}, maximal unloaded shortening velocity determined from the Hill plot; a/P_o, unitless parameter describing curvature of the force–velocity relationship. The relative power unit of watts per litre (W l^{-1}) is equivalent of kN m^{-2} FL s^{-1}; Vel at PP, velocity at peak power; Force at PP, force at peak power; FL, fibre length; no. of high and low treadmill crew members listed in parentheses. *Significantly different from pre-flight value, $P < 0.05$.

Figure 8 shows composite force–power relationships for type I and II fibres of the soleus and gastrocnemius muscles pre- and post-flight. Post-flight peak power of the slow type I and fast type II fibre was significantly depressed in both the soleus and the gastrocnemius (Fig. 8 and Tables 8–10). As shown in Fig. 8, the extent of the decline in peak power of both fibre types was clearly greater in the soleus than the gastrocnemius. Interestingly, while the fast type II fibres from both muscles showed a significant post-flight drop in peak power (μN FL s^{-1}), when corrected for atrophy, the power expressed in watts per litre was only depressed in the fibres isolated from the gastrocnemius. The apparent explanation is that velocity at peak

Journal of Physiology, Vol. 588, No. 18 (September 2010): pg. 3567-3592. DOI.

power was significantly depressed only in gastrocnemius fibres (Table 10).

Table 10. Force-velocity characteristics of fast type II fibres pre- and post-flight

Condition		V_{max}	a/P_0	Peak power			Force at PP	Vel at PP
	n	(FL s^{-1})		(μN FL s^{-1})	(%)	(W l^{-1})	(mN)	(FL s^{-1})
Soleus								
Pre-flight	24	1.76 ± 0.17	0.059 ± 0.005	51.72 ± 4.09		7.37 ± 0.48	0.164 ± 0.011	0.313 ± 0.023
Post-flight	29	1.62 ± 0.14	0.059 ± 0.005	28.52 ± 4.20*	55	6.22 ± 0.56	0.092 ± 0.008*	0.281 ± 0.018
Gastrocnemius								
Pre-flight	58	1.84 ± 0.13	0.079 ± 0.006	40.96 ± 2.80		9.13 ± 0.43	0.117 ± 0.006	0.344 ± 0.016
Post-flight	80	1.68 ± 0.10	0.065 ± 0.005†	32.59 ± 1.44*	80	6.75 ± 0.26*	0.116 ± 0.005	0.292 ± 0.012*

Values are means ± S.E.M.; n, no. of fibres studied. V_{max}, maximal unloaded shortening velocity determined from the Hill plot; a/P_0, unitless parameter describing curvature of the force–velocity relationship. The relative power unit of watts per litre (W l^{-1}) is equivalent of kN m^{-2} FL s^{-1}; Vel at PP, velocity at peak power; Force at PP, force at peak power; FL, fibre length. *Significantly different from pre-flight value, $P < 0.05$; †significantly different from pre-flight value, $P < 0.1$.

Figure 8. Force–power relationship of pre- and post-flight fibres

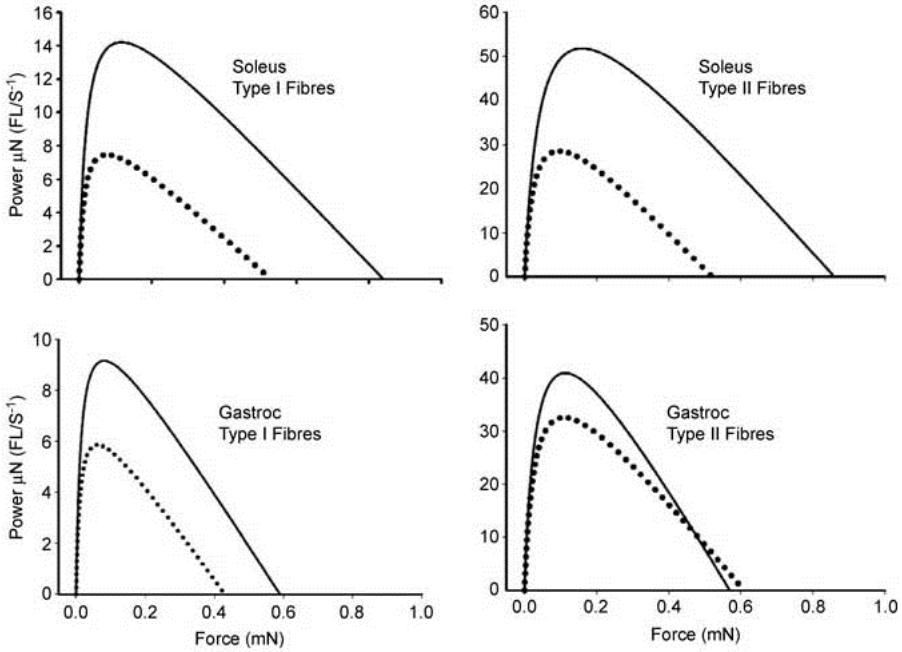

Continuous lines represent composite pre-flight force–power relationships and dashed lines the post-flight composite force–power relationship for soleus type I fibres (upper left), soleus type II fibres (upper right), gastrocnemius type I fibres (lower left), and gastrocnemius type II fibres (lower right).

In the case of the soleus but not the gastrocnemius muscle, the high treadmill grouped showed less loss in type I fibre peak power with a pre/post flight ratio of 63% compared to the low treadmill group mean of 48%. Nine of nine and seven of eight crew members showed a significant ($P < 0.05$) post-flight decline in type I fibre peak power

Journal of Physiology, Vol. 588, No. 18 (September 2010): pg. 3567-3592. DOI.

(μN FL s^{-1}) in the soleus and gastrocnemius, respectively. When these data were expressed as W l^{-1}, the post-flight peak power of the soleus and gastrocnemius type I fibres remained depressed in five and three crew members, respectively (Tables 8 and and9).9). For the majority of crew members, the decline in peak power expressed as W l^{-1} was caused by a significant fall in both the force (mN) and velocity (FL s^{-1}) elicited at peak power (Tables 8 and and99).

The two crew members with the greatest post-flight loss in soleus muscle volume F (−23%) and A (−22%) (see Trappe *et al*. 2009), also showed the greatest soleus type I fibre atrophy (Table 2), and loss of P_0 (Table 3) and absolute peak power (Table 8). Crew member F showed a post-flight increase in peak power in W l^{-1} indicating that for this subject the loss of absolute peak power was entirely explained by the fibre atrophy and the accompanying loss of force. Crew member A who displayed slightly less fibre atrophy and loss of force than crew member F (Tables 2 and and3),3), showed the greatest drop in soleus type I fibre peak power (Table 8). This can be explained in part by a significant decline and increase in the a/P_0 ratio for crew members A and F, respectively (Table 8). Due to the greater curvature of the force–velocity relationship (i.e. lower a/P_0) post-flight, the mean force as a percentage of P_0 at peak power for crew member A's fibres was lower (14% of P_0) than the pre-flight condition (16% of P_0) and this contributed to the reduced power. The opposite was true of crew member F as the a/P_0 ratio for this individual's soleus type I fibres was significantly elevated post-flight (Table 8). In addition, crew member A showed a significant drop in velocity at peak power, while crew member F didn't (Table 8).

Force–pCa relationship

The force–pCa relationship in the slow type I and fast type II fibres pre- and post-flight are shown in Table 11. In the slow but not the fast fibre type, the slope of the Hill plot for values less than half-maximal activation (n_2) were significantly higher post-flight, and this was true for both the soleus and gastrocnemius muscles (Table 11). The pCa_{50} for the slow type I fibre in both muscles showed a small but significant increase (Table 11). The post-flight increase in the n_2 of the type I fibre was not caused by the expression of the fast troponin or

Journal of Physiology, Vol. 588, No. 18 (September 2010): pg. 3567-3592. DOI.

tropomyosin isoforms as SDS gel analysis of the post-flight fibres showed only the cardiac/slow fibre form of troponin C (cTn-C) and the slow isoform of Tn-I, Tn-T and tropomyosin (Fig. 9).

Figure 9. SDS-polyacrylamide gels illustrating MHC, actin, MLC, troponin and tropomyosin in single human soleus fibres

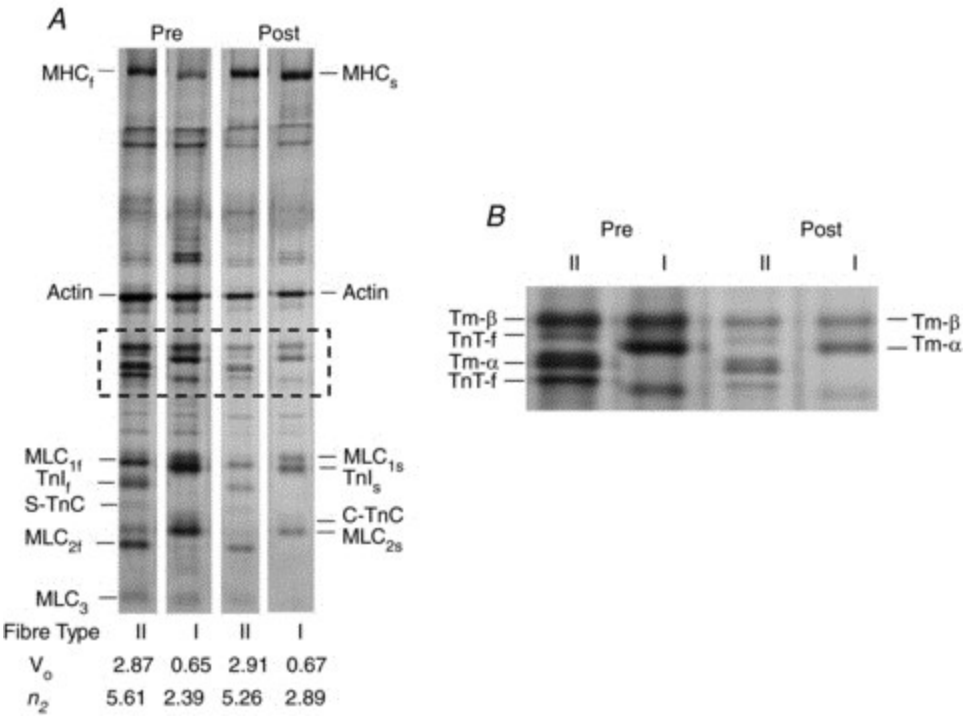

The 12% gel illustrates the protein profile of two pre-flight and two post-flight fibres from crew member F. The fibre type, maximal shortening velocity determined by the slack test (V_0), and the slope of the force–calcium relationship for forces <50% of maximal Ca^{2+}-activated force (n_2) are shown below each lane. The area outlined by the dotted box in panel *A* is expanded in panel *B* to show the troponin T fast fibre isozymes (TnT-f) and the tropomyosin isoforms Tm-β and Tm-α. The latter has a different mobility in fast compared to slow fibres. MHC, myosin heavy chain; MLC, myosin light chain; TnI, troponin I; S-TnC, fast skeletal fibre troponin C; C-TnC, cardiac/slow skeletal troponin C. Slow and fast isoforms of proteins are indicated by subscripted s and f, respectively.

Ultrastructural changes and quantification

At the electron microscopic level, crew members exhibiting high levels of slow fibre atrophy in the soleus muscle following 6 months of spaceflight had smaller myofibrils, fewer intracellular lipids, smaller

Journal of Physiology, Vol. 588, No. 18 (September 2010): pg. 3567-3592. DOI.

and globular mitochondria and increased space between myofibrils filled with glycogen particles (Fig. 10). Conversely, subjects with little atrophy retained similar sized, closely packed myofibrils, lipid droplets and filamentous mitochondria encircling the myofibrils at the I band level (Fig. 10). Within the myofibrils in the A bands after spaceflight, individual thick filaments in the near M band region were surrounded by a greater number of thin filaments compared to pre-flight (Fig. 11). The average thin filament density (2744 ± 167 μm^{-2}) post-flight in the near M region was 22% ($P < 0.01$) higher than that (2253 ± 132 μm^{-2}) before flight. Two subjects did not show high thin filament density post-flight (Fig. 12). The ratio of thin:thick filaments was significantly ($P < 0.01$) higher post-flight (2.9 ± 0.21) compared to pre-flight (2.2 ± 0.15). The increase in thin filaments and amount of fibre atrophy were directly correlated, although the rise in filament density plateaued around 3200 filaments μm^{-2}, indicating an upper limit (Fig. 13). This limit value matches our previously published data (Riley *et al*. 1998, 2000) for thin filament densities in soleus I bands near the Z line, which averaged 3251 μm^{-2} for the two studies (the published density numbers normalized to 2.4 μm were renormalized to 2.5 μm sarcomere length for comparison with current data). The 3251 μm^{-2} represents the largest number nucleated at the Z band (Riley *et al*. 1998, 2000). For the 180-day pre- and post-flight slow fibres, thin filament density and shortening V_0 were inversely related (Fig. 14*A*). In contrast, the mean actin/myosin ratio determined from SDS band densities was unaltered pre- (1.26 ± 0.05) to post-flight (1.29 ± 0.07), and the correlation between the actin/myosin ratios and thin filament densities was not significant (Fig. 14*B*). Of the five crew members showing an increased thin filament density, three showed a small increase and two a small decrease in the actin/myosin ratio post-flight (Fig. 14*B*). The relationship of thin filament density and treadmill use suggested that high treadmill use was partially effective in preventing increased thin filament density (Fig. 15*A*). The level of cycle use also prevented in part the increase in post-flight thin filament density (Fig. 15*B*).

Journal of Physiology, Vol. 588, No. 18 (September 2010): pg. 3567-3592. DOI.

Figure 10. Soleus myofibrillar ultrastructure

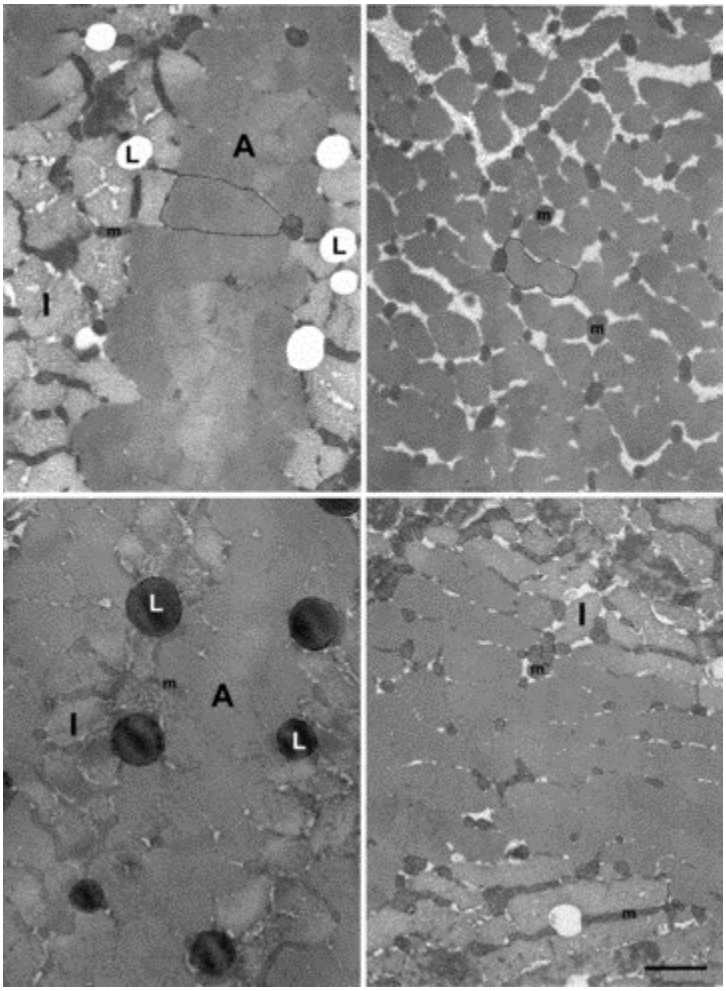

Cross sections of myofibrils cut through the A bands (A) and the thin filament rich I bands (I) in slow fibres of soleus muscle biopsied before and after a 6 month spaceflight from subject F (upper left – pre, upper right – post) averaging 51% atrophy and subject E (lower left – pre, lower right – post) showing moderate atrophy (15%). Myofibrils are outline by dotted lines in the A bands to illustrate decreased size post-flight (upper panels). Myofibrils are not marked in the lower panels because they have indistinct borders typical of slow fibres and are of similar size pre- and post-flight. The filamentous mitochondria (m) predominately encircling I bands in pre-flight muscle fibres become more globular post-flight and invade the A bands, most striking with greater atrophy (upper right). Both subjects contain abundant intracellular lipid droplets (L) pre-flight. Calibration bar, 1.6 μm for all panels.

Journal of Physiology, Vol. 588, No. 18 (September 2010): pg. 3567-3592. DOI.

Figure 11. Soleus thick and thin filament ultrastructure

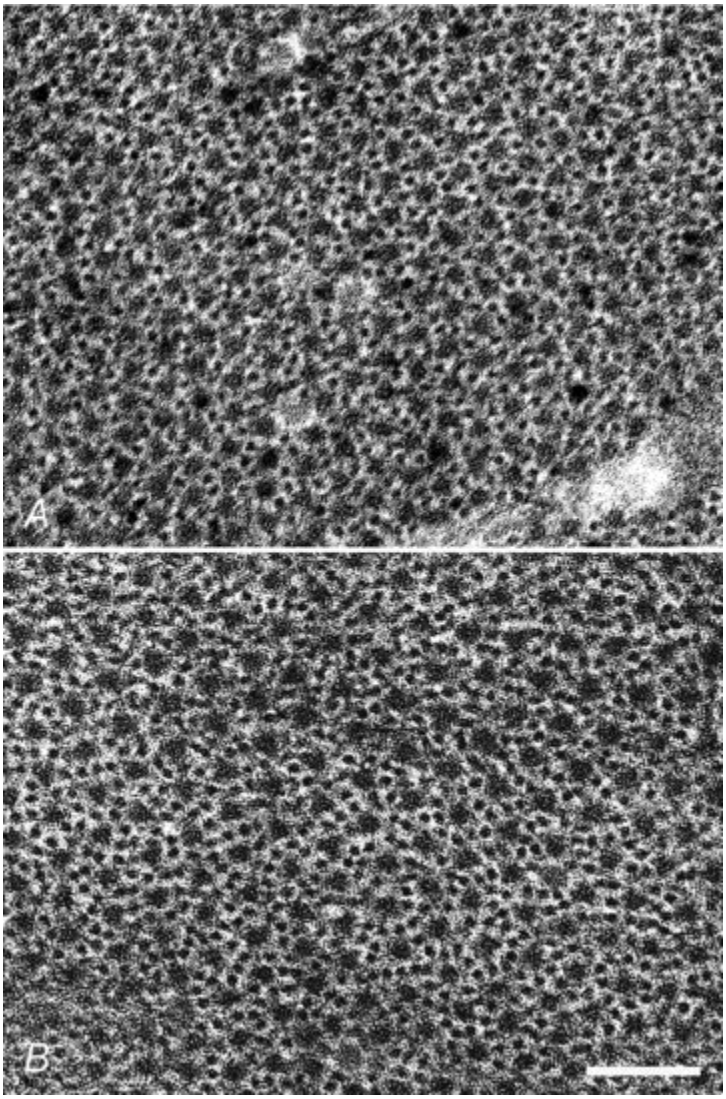

The pre-flight (*A*) and post-flight (*B*) electron microscopic images are cross sections through the A bands in regions showing thick and thin filament overlap in soleus slow fibres from subject F. The near M line region morphometrically sampled is in the centre of each micrograph. The post-flight increase (52%) in thin filament density is readily apparent. Scale bar, 100 nm.

Journal of Physiology, Vol. 588, No. 18 (September 2010): pg. 3567-3592. DOI.

Figure 12. Soleus fibre thin filament density

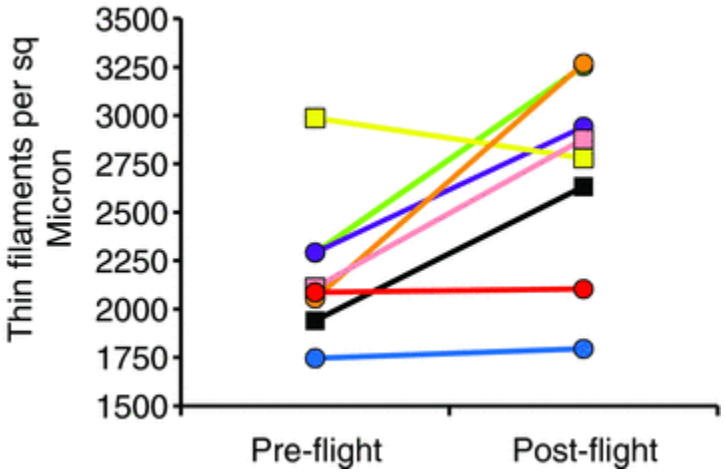

Thin filament density increased post-flight in 5 of 8 crew members and exhibited little change in 3 of 8 crew members. Subjects are colour coded as in Fig. 1. The circles are low treadmill users, and the squares are high treadmill users.

Figure 13. Relationship between soleus fibre atrophy and thin filament density

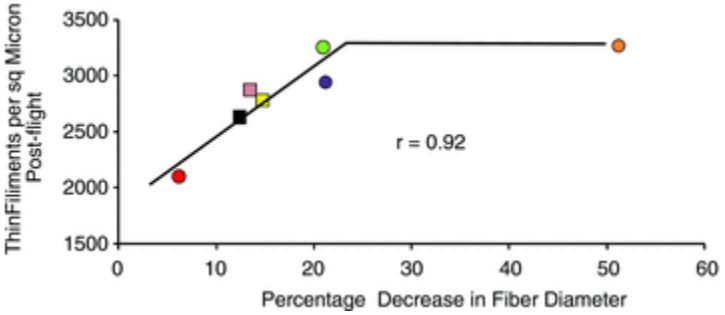

The post-flight increase in thin filament density correlates exponentially ($P < 0.01$) with increasing fibre atrophy. Thin filament density plateaus indicating attainment of the maximum number of thin filaments at ~3200 μm^{-2}. Markers are colour coded as in Fig. 1.

Journal of Physiology, Vol. 588, No. 18 (September 2010): pg. 3567-3592. DOI.

Figure 15. Correlation between thin filament density and the amount of treadmill (*A*) and cycle ergometer (*B*) exercise

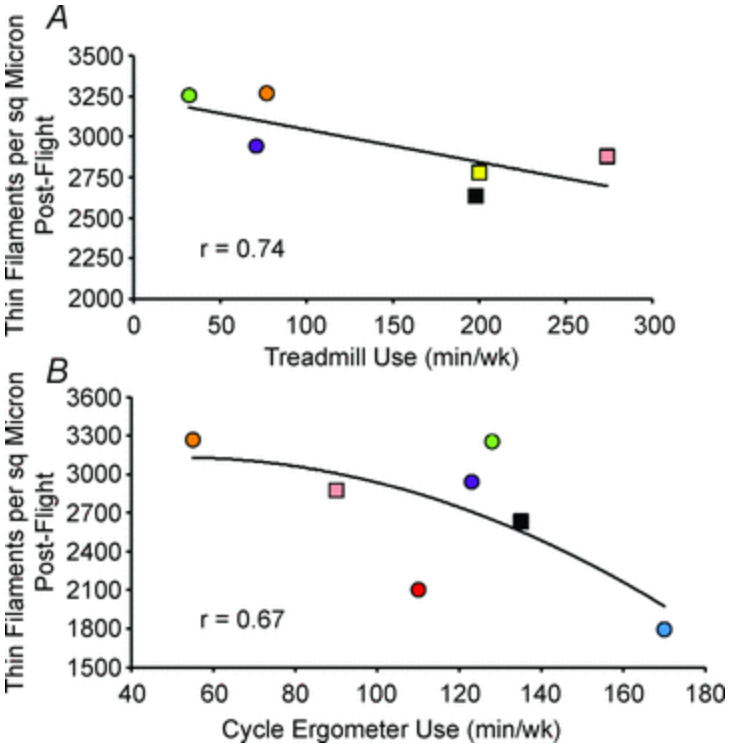

Thin filament density is inversely related ($P < 0.05$) to the amount of treadmill (*A*) and cycle ergometer (*B*) use indicating that high treadmill or cycle ergometer use partially counters the increase in thin filament density. The markers are colour coded for crew member as in Fig. 1.

Discussion

From previous MIR missions and our recent observations on International Space Station crew members, it is well established that significant losses in leg muscle mass occur with prolonged space flight, and that considerable variability in the extent of muscle atrophy exists between individuals (Fitts *et al*. 2000; Trappe *et al*. 2009). The results of this study present the first cellular analysis of the effects of long duration space flight on the structure and function of human skeletal muscle. The main findings were that the prolonged weightlessness produced substantial loss of fibre mass, force and power with the hierarchy of the effects being soleus type I > soleus type II > gastrocnemius type I > gastrocnemius type II. The post-flight decline in power was attributed to declines in both force and velocity.

Journal of Physiology, Vol. 588, No. 18 (September 2010): pg. 3567-3592. DOI.

Structurally, the quantitatively most important adaptation was fibre atrophy, and the resulting loss and shrinkage of myofibrils. An increased packing density of the remaining thick and thin filaments is likely to have contributed to the reduced fibre V_0, increased fibre stiffness and increased cooperativity of force development observed with activation below pCa_{50} in the slow type I fibre types. A final conclusion is that the cellular findings document the inadequacy of the current exercise countermeasures to preserve the pre-flight muscle fibre properties, and point to the need for the development of better exercise protocols and hardware for preventing undesirable transformation of fibre structure and function away from the gravity-loaded adapted state. The primary findings for long-term space flight are discussed with comparison to short duration space flight and prolonged bed rest studies.

Potential limitations of single cell analyses

A major strength of single cell analyses is that spaceflight-induced changes can be assessed in individual fibre types and the impact of structural changes on function determined. A potential limitation is the possibility that the biopsy sample and fibres studied were not fully representative of the changes occurring in the muscles as a whole, and that this might contribute to the diverse range of responses between crew members. However, this seems unlikely for the following reasons. (1) The effects of prolonged space flight on cell atrophy and function tightly reflected the whole muscle changes observed on the same crew for both individual and group responses (Trappe *et al*. 2009). For example, the two crew members with the greatest soleus type I fibre atrophy also lost the most soleus muscle volume detected by MRI. These results are not surprising given the relatively homogeneous nature (88 and 77% slow type I fibres pre- *vs*. post-flight) of the soleus muscle (Trappe *et al*. 2009). In comparison, for the mixed gastrocnemius muscle, the cell atrophy and whole muscle volume loss were not as highly correlated. (2) Confidence that the cell data are representative of the whole muscle is increased by the large number of fibres analysed, which was the largest of any published study. Additionally, separate bundles from the biopsy were studied in two independent labs (Marquette University and Ball State University) and the same results obtained. (3) The soleus type I fibre

Journal of Physiology, Vol. 588, No. 18 (September 2010): pg. 3567-3592. DOI.

atrophy observed in individual fibres and by computerized morphometric analysis of biopsy histochemical cross sections were similar. (4) The soleus muscle is fairly homogeneous (80–90% slow type I), while the gastrocnemius is more of a mixture of slow and fast fibres. Our muscle samples were reflective of these profiles. Taken together these elements provide a reasonable level of support to minimize the size of the muscle sample as a limitation in this study.

Muscle atrophy and fibre force

Consistent with our earlier studies on short-duration space flight (Widrick *et al*. 1999), fibres from the normally tonically active soleus (both slow type I and fast type II) showed greater atrophy than fibres from the phasic gastrocnemius muscle. The 20 and 35% decline in the slow type I fibre diameter and force observed in this work exceeded the 8 and 21% drop in these variables following a 17-day Shuttle flight (Widrick *et al*. 1999) and the 9% atrophy of type I vastus lateralis fibres following an 11-day mission (Edgerton *et al*. 1995). The major cause of the loss in peak force (P_0) was fibre atrophy. The extent of atrophy was documented both at the cell and subcellular level (i.e. reduction in fibre and myofibrillar diameter). The fact that the group mean force per cross-sectional area was unaltered in any fibre type or muscle provides further evidence that the primary cause for the space flight induced loss of muscle and fibre force was fibre atrophy and the accompanying loss in force generating myofilaments. Microgravity-induced fibre atrophy in human muscle is thought to be primarily caused by a reduced protein synthesis (Stein *et al*. 1999; Fitts *et al*. 2000). The molecular mechanism of the decline in muscle protein synthesis is unknown, but at least in rat, models of unloading involve both reduced transcriptional and translational processes (Fitts *et al*. 2000). The observed ~20% increase in fast type II fibres post-flight in some crew members demonstrates that in addition to the downregulation of slow muscle protein that fast muscle myosin isoform was upregulated and that the extent of upregulation was directly related to the degree of fibre atrophy. The signalling mechanism initiating the altered pattern of protein synthesis is likely to be more dependent on the decline in loaded muscle contractions than muscle activity as the latter, at least during short duration space flight, was not altered (Edgerton *et al*. 2001).

Journal of Physiology, Vol. 588, No. 18 (September 2010): pg. 3567-3592. DOI.

Following short duration space flight, we observed a decrease in E_0 and an elevated P_0/E_0 ratio in the slow type I fibre, and hypothesized that the changes may have resulted from the selective loss of the thin (actin) over the thick (myosin) filament (Widrick *et al*. 1999; Riley *et al*. 2000). The resulting increased myofilament lattice spacing may have reduced E_0 (a measure of fibre stiffness) more than P_0 (Kawai & Schulman, 1985; Goldman & Simmons, 1986). With prolonged space flight, we observed just the opposite in that the slow type I fibre E_0 was significantly increased, and the P_0/E_0 ratio decreased post-flight. Since the thin filament density relative to the thick filament density was increased post-flight on average 31% producing a lattice spacing in which the average distance from thick filament cross bridges to the nearest thin filament decreased, we conclude that this closer arrangement increased E_0. Any increase in P_0 that may have resulted from the reduced filament spacing was masked by the large decline in force generated by the fibre atrophy.

Fibre size, exercise, and nutrition

A consistent finding with both short and prolonged duration space flight is that large variability between crew members exists in the extent of muscle atrophy and the commensurate loss in strength. This was particularly true of this study where post-flight soleus type I fibre diameters ranged from 49 to 106% and P_0 from 30 to 90% of the pre-flight values. An unanswered question is what factor(s) caused this variability? It seems likely that a collection of factors to varying degrees contributed, such as initial muscle/fibre size, the type and extent of exercise countermeasures, and nutrition. While it is not possible to assign *post hoc* the relative importance of these factors, our results suggest large influences were the pre-flight fibre size and the pattern of self-selected, exercise countermeasure used. Following short duration space flights, Edgerton & Roy (1996) and our group (Widrick *et al*. 1999) have observed that the greater the pre-flight fibre size the greater was the degree of atrophy post-flight. The present investigation extends that observation to include prolonged space flight. The correlation between pre-flight soleus type I fibre diameter and percentage of fibre atrophy was high (r = 0.87) and very significant (P < 0.001). An obvious conclusion from these observations is that the current exercise countermeasures that emphasize aerobic

Journal of Physiology, Vol. 588, No. 18 (September 2010): pg. 3567-3592. DOI.

exercise (see Trappe *et al*. 2009 for a detailed description on the ISS exercise countermeasure programme) fail to protect muscle mass, and this is particularly true for the antigravity soleus muscle. It is clear that the resistance exercises employed on the ISS during Increments 5–9 utilized low intensity devices incapable of providing the high-intensity needed to adequately protect fibre and muscle mass (Trappe *et al*. 2009). The aerobic exercise used on the ISS provided detectable partial preservation of pre-flight properties when crew members utilized the treadmill modality >200 min week^{-1}. There was less fibre atrophy, loss of force and increase in thin filament density than for crew members who performed less than 100 min week^{-1} of treadmill exercise. Relying more on the cycle ergometer did not appear to make up for low treadmill usage, although additional controlled comparisons are necessary. For example, subject A cycled >30 min more per week than the nine crew member average (Trappe *et al*. 2009) but sustained the second largest decline in soleus type I fibre diameter and P_0. On the other hand, this subject exhibited the greatest prevention of thin filament density increase. The level of cycle use and the level of treadmill use both correlated highly with prevention of post-flight increase in thin filament density. The relative lack of protection of soleus muscle mass with cycling is likely to reflect the fact that this muscle is only activated during a small portion of the pedalling cycle (Gregor *et al*. 1991). In the case of ameliorating thin filament density (length), it may be the stretch (muscle lengthening) stimulation during treadmill walking and cycle pedalling that is preventative. While our data suggest that treadmill exercise in excess of 200 min week^{-1} can in part compensate for the lack of an effective high intensity exercise device, this conclusion must be interpreted with caution as the high treadmill group with less fibre atrophy also had a smaller mean pre-flight soleus type I fibre diameter (Table 2). In all likelihood, high treadmill use and smaller pre-flight fibre size both contributed to the relative protection of the high treadmill group. Based on pre-flight conditioning biographies (Trappe *et al*. 2009) and soleus type I fibre aerobic enzyme content (unpublished data), the in-flight low treadmill group were in better aerobic condition at the start of the mission compared to the high treadmill group. Thus, the greater decline in fibre size and force of the low treadmill group is likely to reflect the combined effects of greater initial fitness (both aerobic and strength), and the ineffectiveness of the in-flight exercise

Journal of Physiology, Vol. 588, No. 18 (September 2010): pg. 3567-3592. DOI.

countermeasures. Presumably, with a better in-flight high resistance training device, crew members would be able to maintain muscle mass and strength gained through pre-flight exercise programmes.

Previous investigations have documented that voluntary energy intake is reduced in microgravity, and that as a result many crew members have been found to be in negative nitrogen balance (Stein *et al*. 1999). While the focus of this study was not nutrition, we calculated from the nutritional profile and weekly exercise that the caloric intake of the crew members we studied was ~20% below the predicted need (Trappe *et al*. 2009). Clearly, an insufficient dietary intake could limit protein synthesis induced by exercise and activate muscle catabolism (Stuart *et al*. 1990; Paddon-Jones *et al*. 2004).

k_{tr} and fibre velocity

The rate constant of tension redevelopment of an isometric contraction (k_{tr}) is thought to be the sum of the rate constant for attachment (k^+) and detachment (k^-) of the cross-bridges and reflect the transition from the weak (low force) to the strong (high force) cross-bridge state (Brenner, 1991; Metzger & Moss, 1990; Fitzsimons *et al*. 2001). Brenner (1991) reported that k^+ and k^- were an order of magnitude greater than the rate constants for cross-bridge turnover (f_{app} and g_{app}). Thus while k_{tr} and V_0 are known to be correlated across fibre type and species (Gordon *et al*. 2000), it seems unlikely that they are limited by the same molecular step in the cross-bridge cycle. The published values for k_{tr} range from 3 to 23 s^{-1} for slow and fast rat fibres with the rabbit psoas ~16 s^{-1} (Metzger & Moss, 1990; Fitzsimons *et al*. 2001). The k_{tr} has been shown to have a high Ca^{2+} dependency increasing 10-fold as Ca^{2+} increases from just threshold to levels eliciting maximal force. Our measurements were made at saturating levels of Ca^{2+} such that the mean k_{tr} of ~1.5 for the slow type I fibres of the soleus and the gastrocnemius reflects the maximal value for slow type I human fibres. The slow type I fibre k_{tr} of ~1.5 is one-half that reported for comparable rat fibres, but this is consistent with the known decline in this variable with increased species body size (Gordon *et al*. 2000), and with the data of Köhler *et al*. (2002) for human soleus fibres. Recent observations of Moreno-Gonzalez *et al*. (2007) suggest that in addition to a Ca^{2+} dependency, k_{tr} is affected by

the isoform of troponin C (Tn-C). Fast fibres reconstituted with slow Tn-C (the cardiac isoform) showed a significant decline in k_{tr}. The observation in this study that slow type I fibre k_{tr} was not different pre- to post-flight is consistent with the detection of only slow troponin in both pre- and post-flight slow fibres, and suggests that space flight had no effect on the kinetics of the transition from the low to the high force state.

Fibre V_0, thought to reflect the cross-bridge cycle speed, was depressed by ~20% in all fibre types except the soleus fast type II fibre. The mechanism responsible for the depressed V_0 is not obvious, and could not be attributed to an altered myosin heavy or light chain pattern. While some subjects experienced a phenotype switch in the soleus from slow to fast that approached 20%, the post-flight fibres identified as type I contained only the slow myosin isoform. While it seems unlikely, the possibility exists that space flight triggered a post-translational modification of myosin or the expression of a second slow isoform of myosin that went undetected by the SDS gel analysis (Fauteck & Kandarian, 1995; Galler *et al*. 1997). The flight-induced depression of V_0 is in contrast to short duration space flight where we observed an average increase of 30% in the soleus type I fibre V_0 (Widrick *et al*. 1999). We attributed the elevated V_0 in the short duration flight to a selective loss in thin filaments (actin) and the resulting increase in lateral distance between the thin and thick filaments, and hypothesized that this stereological change caused the cycling myosin head to detach from the actin earlier reducing the internal drag and accelerating velocity (Widrick *et al*. 1999). In our rat 14 day hindlimb suspension unloading study, the soleus V_o increased and correlated with decreased thin filament density (Riley *et al*. 2005). When the soleus fibre myofilament lattice was compacted by 5% dextran, V_o slowed from 1.370 to 0.959 FL s^{-1} substantiating that increasing myofilament packing density has a profound slowing effect on shortening velocity (Riley *et al*. 2005). These results are consistent with the lower V_{max} observed by dextran treatment in rat soleus fibres (Metzger & Moss, 1987). The current data suggest that the selective loss in actin with short duration space flight was a non-steady state transitional effect. With prolonged space flight, where it is reasonable to assume that crew members have adapted to a microgravity steady state, we found increased thin filament density surrounding thick filaments. This structural change would be expected to increase

Journal of Physiology, Vol. 588, No. 18 (September 2010): pg. 3567-3592. DOI.

internal drag and reduce fibre V_0. This effect was not an exclusive factor as two crew members showed a significant decline in soleus type I fibre V_0 with no change in thin filament density.

The total number of thin filaments is regulated by a finite number of nucleating sites (α-actinin, CapZ) per cross-sectional area of Z band (Castillo *et al*. 2009; Littlefield & Fowler, 2008). What accounted for the increase in thin filament density in the present study? The answer was increased length of thin filaments. The numbers of thin filaments were counted in the Near M region an area of the A band into which only long thin filaments can reach at a sarcomere length of 2.5 μm (Fig. 16). Compared to pre-flight, the thin filament number increased by 22%. The post-flight packing density in the near M region (2744 ± 167 μm^2) approached the level in the I bands (near the Z line) of pre-bedrest (2932 ± 186 μm^2) and pre-17-day spaceflight (3569 ± 236 μm^2) slow soleus fibres (Riley *et al*. 1998, 2000). The concepts of thin filament growth in length and increased thin filament density near the M region are shown schematically in Fig. 16. The density of thin filaments increased in five of eight crew members analysed following 6 months in space (Fig. 12). Despite the significant increase in thin filament density, the average actin/myosin ratio pre- to post-flight was unaltered. This suggests that actin/myosin ratio determined from a whole fibre segment lacked the sensitivity to detect relatively small changes in thin filament density at the Near M region. An alternative explanation is that the fibres tested for thin filament density may not have been representative of the whole muscle. Recent studies suggest that the dynamic nature of thin filament length in skeletal muscle is regulated by tropomodulin capping of the pointed end (closest to the M line) influenced by titin and nebulin isoforms (Prado *et al*. 2005; Littlefield & Fowler, 2008; Castillo *et al*. 2009). Examining these proteins will be of great importance for future spaceflight studies.

The present investigation, the 17-day flight study, and our rat study show that thin filament density relative to thick filament density can modulate shortening velocity (Riley *et al*. 1998, 2005). What stimulated the increase in thin filament density (length)? Higher thin filament density correlated directly with increased fibre atrophy. However, atrophy *per se* does not modulate thin filament packing density because the soleus and adductor longus (AL) muscles of the

rat both atrophied 50–60% during hindlimb suspension unloading but only the soleus exhibited reduced thin filament density (Riley *et al*. 2005). The difference was that soleus was also shortened by plantarflexion foot-drop posture, whereas AL was only unloaded. Since Skylab missions, it has been noted that crew members assume a plantarflexion foot-drop posture when floating in reduced gravity (Thornton, 1978; Clement & Lestienne, 1988). The ankle angle plantarflexion progressively increased during the first 7 days of spaceflight and was plateaued at 45 days (Thornton, 1978; Clement & Lestienne, 1988). Adaptation of muscle to working or operating range of motion has been shown in humans and animal models to modulate the number of in-series sarcomeres (Witzmann *et al*. 1982; Burkholder & Lieber, 2001; Riley *et al*. 2002). This optimizes muscle length to generate maximum tension (optimal thick thin filament overlap). The reduction in sarcomere number in response to the microgravity-induced plantarflexion takes days and is likely to be complete by 1 month in space. Adaptation of the calf muscles to a shortened posture may explain why at 17 days of space flight we found decreased thin filament density (length) and increased shortening velocity (Riley *et al*. 1998). With long duration spaceflight, the relatively short daily exercises optimized to maintain endurance and to a much lesser extent preserve mass were not robust enough or performed over a wide enough range of motion to counter the microgravity-induced calf shortening by stimulating regrowth of in-series sarcomeres. However, the treadmill, cycle ergometer and iRED heal raises introduced some contractions of the calf muscles while in a lengthened position. Such contractions would have stretched the sarcomeres, and this may have triggered thin filament growth in length. The resulting longer thin filament length (density) was correlated with and is likely to have contributed to the slowing of fibre shortening velocity in 6 of 9 subjects. Variations in thin filament length have been postulated to optimize thin and thick filament overlap (length tension properties) to meet the range of motion the workload demands (Littlefield & Fowler, 2008). Thus it appears that the exercise prescription could be improved by introducing a higher resistance calf muscle contractions over a wider range of motion (particularly long lengths) such that the muscles function over the full range of motion as occurs in Earth's 1 *g* environment. We hypothesize that this would reduce the microgravity-induced decline in muscle mass and prevent calf plantarflexion. This

Journal of Physiology, Vol. 588, No. 18 (September 2010): pg. 3567-3592. DOI.

concept requires validation testing on ISS with a more tightly defined and standardized exercise protocol than was available for the present study.

The observed decline in type I fibre V_0 (soleus and gastrocnemius muscles) was similar to the data of Trappe *et al*. (2004) who found an ~20% drop in the V_0 type I vastus lateralis fibres following 84 days of bed rest in subjects who performed no exercise countermeasures. In contrast, Yamashita-Goto *et al*. (2001) reported a 2-fold increase in the V_0 of soleus type I fibres following 4 months of bed rest without exercise. In the Trappe *et al*. (2004) study, a high resistance exercise countermeasure completely prevented the decline in V_0. The authors hypothesized that unloading with no exercise induces a decline in type I fibre V_0, while with exercise countermeasure programmes, type I fibre V_0 is elevated. A comparison of our short and prolonged duration space flight studies, both of which employed exercise countermeasures, suggests that the situation is more complex. Clearly, fibre V_0 changes with unloading are dependent not only on the exercise countermeasure (amount of resistance and lengthening contractions) but the duration of unloading. Unlike fibre diameter and force, the effect of space flight on fibre V_0 was not different in the low and high treadmill exercisers as both groups showed the same decline. It is clear that the exercise countermeasure used on the ISS did not prevent the decline in fibre V_0.

Fibre power

The post-flight peak power was depressed in all fibre types and both muscles studied, and with the exception of crew member F, the decline was greater than that observed for peak force. By far the greatest contributor to the loss of peak power in all but the fast type II gastrocnemius fibres was atrophy and the resulting loss of force. For example, the post-flight soleus slow type I fibre developed only 54% of the peak power obtained pre-flight. When corrected for CSA (expressed as W l^{-1}) this increased to 87%. The fast type II fibres from the gastrocnemius were an exception in that force was not altered and the 20% drop in post-flight peak power was attributed to a reduced velocity.

Journal of Physiology, Vol. 588, No. 18 (September 2010): pg. 3567-3592. DOI.

Unlike short duration space flight where the soleus type I fibre power was partially protected by increases in the velocity obtained, power fell dramatically, and for most of the crew this was due to a loss of both the force and velocity obtained during the generation of peak power. One exception was crew member F where, despite the largest decline in peak force (P_0) and maximal velocity (V_0), the type I fibre showed no significant drop in velocity at peak power due to a reduced curvature of the force–velocity relationship as reflected by the significant increase in the post-flight a/P_0 ratio. As a result, the post-flight soleus type I fibres of crew member F shortened at a velocity that on average was 21% of V_0. In comparison, the post-flight soleus type I fibres from crew member A showed a significant decline in the a/P_0 ratio, and maintained only 14% of V_0 at peak power. The combined loss of force and velocity reached at peak power resulted in the greatest decline in peak power (28% of pre-flight) observed for any of the nine crew members.

The average drop in peak power for the soleus type I fibre with weightlessness was of a similar magnitude to that observed for the vastus lateralis type I fibres with 84 days of bed rest without countermeasures (54 *vs*. 45% of pre-unloading value). However, the type I fibres in the bed rest countermeasure group maintained 71% of their pre-bed rest power (Trappe *et al*. 2004). It is apparent that the high resistance exercise, and possibly the range of motion, employed in the bed rest study was more effective in protecting fibre mass, force and power than that used on the ISS. A major difference between prolonged bed rest and space flight is the observation that the former had no effect on type II fibre peak power, while this parameter was equally depressed with space flight in the type I and II fibres of the soleus.

Calcium sensitivity

In agreement with previous short and long duration bed rest and short duration space flight studies, the calcium sensitivity as reflected by the force–pCa relationship was rather resistant to unloading induced changes (Stevens *et al*. 1993; Widrick *et al*. 1998, 1999; Yamashita-Goto *et al*. 2001). While short and long duration bed rest has been shown to slightly increase the Ca^{2+} required for one-half

Journal of Physiology, Vol. 588, No. 18 (September 2010): pg. 3567-3592. DOI.

maximal activation, we observed either no change or a slight decrease (elevated pCa) in this parameter with short and long term space flight, respectively. While short duration space flight had no effect on the slope of the force–pCa relationship for Ca^{2+} values below pCa_{50} (n_2), this parameter was significantly increased following long duration. The effect was not caused by an increased expression of the fast isoform of troponin or tropomyosin.

In conclusion, the results of this study clearly illuminate the deleterious effects of prolonged space flight on the structure and function of both slow type I and fast type II fibres of the calf muscle group. The extensive decline in peak force and power can be largely attributed to cell atrophy and the accompanying loss of myofilaments. The restructuring elongation of the thin filaments causing increased thin filament density appears to be of major importance to the depressed fibre velocity a factor that exacerbates the decline in peak power. This work highlights the extensive nature of the weightlessness induced muscle remodelling and loss of peak power in all fibre types, and the limitations of the current ISS exercise countermeasure programme with its focus on light to moderate intensity (Trappe *et al*. 2009). Clearly, the deleterious changes in muscle structure and function with prolonged space flight documented in this study have potentially serious implications for a variety of circumstances including but not limited to the crew's ability to perform an emergency egress; muscle damage due to high force particularly eccentric contractions; and difficulties performing work on the surface of the moon or Mars. Bed rest studies show that high resistance exercise countermeasure programmes are effective and time efficient. Employing similar well controlled and standardized exercise investigations on the ISS, documenting their effectiveness, and monitoring crew member nutritional status to insure an adequate caloric intake should be the high priorities that fulfils the intended scientific use of the spacecraft.

Acknowledgments

We thank the astronauts and cosmonauts who graciously gave their time and energy to this research. We thank Simone Thomas, Elkin Romero, Alicia Forrester, the flight surgeons, and the numerous unnamed people who assisted our research team at the National Aeronautics and Space Administration (NASA) and Russian Space

Agencies. This research was supported by a National Aeronautics and Space Administration Grant NCC9-116 to R.H.F.

Glossary

Abbreviations

CSA cross-sectional area
FL fibre length
ISS International Space Station
k_{tr} rate constant of tension redevelopment
P_0 peak force
V_0 maximal unloaded shortening velocity

Author contributions

Authors R.H.F., S.W.T., D.L.C., and D.A.R. all participated in the conception and design of the experiments, analysis and interpretation of data, drafting, revision and final approval of the article. Authors P.M.G., A.C.C., P.A.C., J.R.P., J.G.R. all participated in analysis and interpretation of the data.

References

Antonutto G, Capelli C, Girardis M, Zamparo P, di Prampero PE. Effects of microgravity on maximal power of lower limbs during very short efforts in humans. J Appl Physiol. 1999;86:85–92.

Bergstrom J. Muscle electrolytes in man. Scand J Clin Lab Invest. 1962;14(Suppl 68):7–110.

Brenner B. Rapid dissociation and reassociation of actomyosin cross-bridges during force generation: A newly observed facet of cross-bridge action in muscle. Proc Natl Acad Sci U S A. 1991;88:10490–10494.

Burkholder TJ, Lieber RL. Sarcomere length operating range of vertebrate muscles during movement. J Exp Biol. 2001;204:1529–1536.

Castillo A, Nowak R, Littlefield KP, Fowler VM, Littlefield RS. A nebulin ruler does not dictate thin filament lengths. Biophys J. 2009;96:1856–1865.

Clement G, Lestienne F. Adaptive modifications of postural attitude in conditions of weightlessness. Exp Brain Res. 1988;72:381–389.

Convertino VA. Physiological adaptations to weightlessness: effects on exercise and work performance. Exerc Sports Sci Rev. 1990;18:119–166.

Edgerton VR, McCall GE, Hodgson JA, Gotto J, Goulet C, Fleischmann K. Sensorimotor adaptations to microgravity in humans. J Exp Biol. 2001;204:3217–3224.

Edgerton VR, Roy RR. Handbook of Physiology, *section 4* Environmental Physiology. II. Bethesda, MD: American Physiological Society; 1996. Neuromuscular adaptations to actual and simulated spaceflight; pp. 721–763. Chap 32.

Edgerton VR, Zhou M-Y, Ohira Y, Klitgaard H, Jiang B, Bell G, Harris B, Saltin B, Gollnick PD, Roy RR, Day MK, Greenisen M. Human fiber size and enzymatic properties after 5 and 11 days of spaceflight. J Appl Physiol. 1995;78:1733–1739.

Fabiato A, Fabiato F. Calculator programs for computing the composition of the solutions containing multiple metals and ligands used for experiments in skinned muscle cells. J Physiol (Paris) 1979;75:463–505.

Fauteck SP, Kandarian SC. Sensitive detection of myosin heavy chain composition in skeletal muscle under different loading conditions. Am J Physiol Cell Physiol. 1995;268:C419–C424.

Fitts RH, Riley DR, Widrick JJ. Microgravity and skeletal muscle. J Appl Physiol. 2000;89:823–839.

Fitts RH, Riley DR, Widrick JJ. Functional and structural adaptations of skeletal muscle to microgravity. J Exp Biol. 2001;204:3201–3208.

Journal of Physiology, Vol. 588, No. 18 (September 2010): pg. 3567-3592. DOI.

Fitts RH, Romatowski JG, Peters JR, Paddon-Jones D, Wolfe RR, Ferrando AA. The deleterious effects of bed rest on human skeletal muscle fibers are exacerbated by hypercortisolemia and ameliorated by dietary supplementation. Am J Physiol Cell Physiol. 2007;293:C313–C320.

Fitzsimons DP, Patel JR, Campbell KS, Moss RL. Cooperative mechanisms in the activation dependence of the rate of force development in rabbit skinned skeletal muscle fibers. J Gen Physiol. 2001;117:133–148.

Galler S, Hilber K, Gohlsch B, Pette D. Two functionally distinct myosin heavy chain isoforms in slow skeletal muscle fibres. FEBS Lett. 1997;410:150–152.

Godt RE, Lindley BD. Influence of temperature upon contractile activation and isometric force production in mechanically skinned muscle fibers of the frog. J Gen Physiol. 1982;80:279–297.

Goldman YE, Simmons RM. The stiffness of frog skinned muscle fibres at altered lateral filament spacing. J Physiol. 1986;378:175–194.

Gordon AM, Homsher E, Regnier M. Regulation of contraction in striated muscle. Physiol Rev. 2000;80:853–924.

Gregor RJ, Broker JP, Ryan MM. The biomechanics of cycling. Exerc Sports Sci Rev. 1991;19:127–169.

Huckstorf BL, Slocum GR, Bain JLW, Reiser PM, Sedlak FR, Wong-Riley MTT, Riley DA. Effects of hindlimb unloading on neuromuscular development of neonatal rats. Brain Res Dev Brain Res. 2000;119:169–178.

Kawai M, Schulman MI. Crossbridge kinetics in chemically skinned rabbit psoas fibres when the actin-myosin lattice spacing is altered by dextran T-500. J Mus Res Cell Motil. 1985;6:313–332.

Köhler J, Winkler G, Schulte I, Scholz T, McKenna W, Brenner B, Kraft T. Mutation of the myosin converter domain alters cross-bridge elasticity. Proc Natl Acad Sci U S A. 2002;99:3557–3562.

Littlefield RS, Fowler VM. Thin filament length regulation in striated muscle sarcomeres: pointed-end dynamics go beyond a nebulin ruler. Semin Cell Dev Biol. 2008;19:511–519.

Metzger JM, Moss RL. Shortening velocity in skinned single muscle fibers influence of filament lattice spacing. Biophys J. 1987;52:127–131.

Metzger JM, Moss RL. pH modulation of the kinetics of a Ca^{2+}-sensitive cross-bridge state transition in mammalian single skeletal muscle fibres. J Physiol. 1990;428:751–764.

Moreno-Gonzalez A, Gillis TE, Rivera AJ, Chase PB, Martyn DA, Regnier M. Thin-filament regulation of force redevelopment kinetics in rabbit skeletal muscle fibres. J Physiol. 2007;579:313–326.

Moss RL. Sarcomere length-tension relations of frog skinned muscle fibres during calcium activation at short lengths. J Physiol. 1979;292:177–192.

Paddon-Jones D, Sheffield-Moore M, Urban RR, Sanford AP, Aarsland A, Wolfe RR, Ferrando AA. Essential amino acid and carbohydrate supplementation ameliorates muscle protein loss in humans during 28 days bedrest. J Clin Endocrinol Metabol. 2004;89:4351–4358.

Prado LG, Makarenko I, Andresen C, Kruger M, Opitz CA, Linke WA. Isoform diversity of giant proteins in relation to passive and active contractile properties of rabbit skeletal muscles. J Gen Physiol. 2005;126:461–480.

Riley DA, Bain JLW, Thompson JL, Fitts RH, Widrick JJ, Trappe SW, Trappe TA, Costill DL. Disproportionate loss of thin filaments in human soleus muscle after 17-day bed rest. Muscle Nerve. 1998;21:1280–1289.

Riley DA, Bain JLW, Thompson JL, Fitts RH, Widrick JJ, Trappe SW, Trappe TA, Costill DL. Decreased thin filament density and length in human atrophic soleus muscle fibres after spaceflight. J Appl Physiol. 2000;88:567–572.

Riley DA, Bain JL, Thompson JL, Fitts RH, Widrick JJ, Trappe SW, Trappe TA, Costill DL. Thin filament diversity and physiological properties of fast and slow fiber types in astronaut leg muscles. J Appl Physiol. 2002;92:817–825.

Riley DA, Bain JL, Romatowski JG, Fitts RH. Skeletal muscle fiber atrophy: altered thin filament density changes slow fiber force and shortening velocity. Am J Physiol Cell Physiol. 2005;288:C360–365.

Schakel SF, Sievert YA, Buzzard IM. Sources of data for developing and maintaining a nutrient database. J Am Diet Assoc. 1988;88:1268–1271.

Smith S, Zwart S. Nutritional biochemistry of spaceflight. Adv Clin Chem. 2008;46:87–130.

Stein TP, Leskiw MJ, Schluter MD, Donaldson MR, Larina I. Protein kinetics during and after long-duration spaceflight on MIR. Am J Physiol Endocrinol Metab. 1999;276:E1014–E1021.

Stuart CA, Shangraw RE, Peters EJ, Wolfe RR. Effect of dietary protein on bed-rest related changes in whole-body-protein synthesis. Am J Clin Nutri. 1990;52:509–514.

Stevens L, Mounier Y, Holy X. Functional adaptation of different rat skeletal muscles to weightlessness. Am J Physiol Regul Integr Comp Physiol. 1993;264:R770–R776.

Thornton W. Anthropometry for Designers. 1978. Anthropometric changes in weightlessness. ed. Staff of Anthropology Research Project and Webb Associates, Yellow Springs, OH, Chap I, pp. I1–I60. NASA Reference Publication 1024, Anthropometric Source Book, vol I, Accession Number: 79N11734; Document

ID: 19790003563; Report Number: NASA-RP-1024, S-479-VOL-1.

Trappe T, Costill D, Gallagher P, Creer A, Peters JR, Evans H, Riley DA, Fitts RH. Exercise in space: human skeletal muscle after 6 months aboard the international space station. J Appl Physiol. 2009;106:1159–1168.

Trappe S, Trappe T, Gallagher P, Harber M, Alkner B, Tesch P. Human single muscle fibre function with 84 day bed-rest and resistance exercise. J Physiol. 2004;557:501–513.

Widrick JJ, Knuth ST, Norenberg KM, Romatowski JG, Bain JLW, Riley DA, Karhanek M, Trappe SW, Trappe TA, Costill DL, Fitts RH. Effect of a 17 day spaceflight on contractile properties of human soleus muscle fibres. J Physiol. 1999;516:915–930.

Widrick JJ, Norenberg KM, Romatowski JG, Blaser CA, Karhanek M, Sherwood J, Trappe SW, Trappe TA, Costill DL, Fitts RH. Force-velocity-power and force-pCa relationships of human soleus fibers after 17 days of bed rest. J Appl Physiol. 1998;85:1949–1956.

Widrick JJ, Romatowski JG, Bain JLW, Trappe SW, Trappe TA, Thompson JL, Costill DL, Riley DA, Fitts RH. Effect of 17 days of bed rest on peak isometric force and unloaded shortening velocity of human soleus fibers. Am J Physiol Cell Physiol. 1997;273:C1690–C1699.

Witzmann FA, Kim DH, Fitts RH. Hindlimb immobilization: length-tension and contractile properties of skeletal muscle. J Appl Physiol. 1982;53:335–345.

Yamashita-Goto K, Okuyama R, Honda M, Kawasaki K, Fujita K, Yamada T, Nonaka I, Ohira Y, Yoshioka T. Maximal and submaximal forces of slow fibers in human soleus after bed rest. J Appl Physiol. 2001;91:417–424.

Zange J, Muller K, Schuber M, Wackerhage H, Hoffmann U, Gunther RW, Adam G, Neuerburg JM, Sinitsyn VE, Bacharev AO,

Belichenko OI. Changes in calf muscle performance, energy metabolism, and muscle volume caused by long term stay on space station MIR. Int J Sports Med. 1997;18:S308–S309.